ICARUS **127,** 354–378 (1997)
ARTICLE NO. IS965663

Near-Infrared Spectroscopy of Simple Hydrocarbons and Carbon Oxides Diluted in Solid N_2 and as Pure Ices: Implications for Triton and Pluto

Eric Quirico and Bernard Schmitt

Laboratoire de Glaciologie et Géophysique de l'Environnement, CNRS, associé à l'Université Joseph Fourier, 54 rue Molière, B.P. 96,
38402 Saint Martin d'Hères Cedex, France
E-mail: quiri@glaciog.grenet.fr

Received June 19, 1995; revised November 27, 1996

In this paper are presented near-infrared laboratory spectra of pure ices of CH_4, C_2H_4, C_2H_6, CO, and CO_2, as well as a systematic study of changes in their spectral behavior when isolated in a matrix of nitrogen ice. These studies were prompted by recent low-noise and high-spectral-resolution infrared observations of the surfaces of Triton and Pluto (e.g., D. P. Cruikshank *et al.,* 1993, *Science* 261, 742–745; T. C. Owen *et al., Science* 261, 745–748). The data in this paper permit a sophisticated analysis of the published Pluto and Triton spectra, and will be useful in interpreting future observations as well. Two different techniques were employed for preparing our ice samples: (1) condensation of thin films on a cold window, and (2) growth of crystals from the liquid phase in a closed cryogenic cell. An important result we obtained is that spectra strongly depend on the technique used. With a closed cell, samples are formed under conditions of thermodynamical equilibrium and experiments are perfectly reproducible. Additionally, the samples formed from mixtures of N_2 and CH_4, in the closed cell, show characteristics consistent with the N_2:CH_4 phase diagram obtained by A. I. Prokhvatilov and L. D. Yantsevich (1982, *Sov. J. Low Temp. Phys.* 9, 94–98). On the other hand, it appeared that this is not at all the case with thin films. Assuming that the surfaces of Triton and Pluto are in thermodynamical equilibrium, the closed cell technique is more appropriate. Finally, the measurements conducted with different closed cryogenic cells show that the peak frequencies of the bands of the CH_4 molecule isolated in solid N_2 are shifted with respect to pure CH_4 ice and are also dependent on the temperature and crystal phase of solid N_2 (α vs β). These dependencies have been precisely measured, and it is shown how they could be used to determine the CH_4 dilution state and the temperature at the surfaces of Triton and Pluto to higher precision than has been previously achieved. © 1997 Academic Press

1. INTRODUCTION

The development of powerful infrared detectors has permitted new infrared observations of icy surfaces of satellites or planets at high spectral resolution (~1 cm^{-1}) and high signal/noise ratio, allowing numerous spectrally resolved absorption bands to be observed. These observations are very rich from the chemicophysical point of view, but need a complex and rigorous analysis to extract all the information they contain. In particular, this analysis depends on laboratory experiments: first, to determinate the spectral identity of ices or mixtures suspected to be present on the observed icy surface, allowing identification of molecules, and second, to seek chemicophysical indicators permitting extraction of specific parameters such as temperature and dilution state (for more details, see Quirico *et al.* 1996).

In the cases of Triton and Pluto, observations with high spectral resolution have been obtained during recent years and their analysis awaits specific laboratory experiments. Cruikshank *et al.* (1993) and Owen *et al.* (1993), in part on the basis of some data contained in this paper, identified new molecules on the surfaces of Triton (CO, CO_2) and Pluto (N_2, CO), and furthermore gave information about the physical state of some molecules. In particular, these authors found that the positions of the CH_4 bands contained in the spectra were all shifted with respect to pure CH_4 ice, and have interpreted this shift as indicating this molecule is diluted in solid N_2.

The aim of this paper is to present some useful experimental data for the analysis of spectra of icy surfaces, especially those of Triton and Pluto. In the first step, we describe in detail the experimental and, more precisely, the optical cells specifically designed and built to grow thick icy crystals. We then present laboratory spectra of the CH_4, C_2H_4, C_2H_6, CO, and CO_2 molecules diluted in solid nitrogen and as pure ices.

Next, we present a systematic study of the effect of temperature and concentration on the spectrum of the CH_4 molecule diluted in solid N_2 at low concentrations (from

0019-1035/97 $25.00

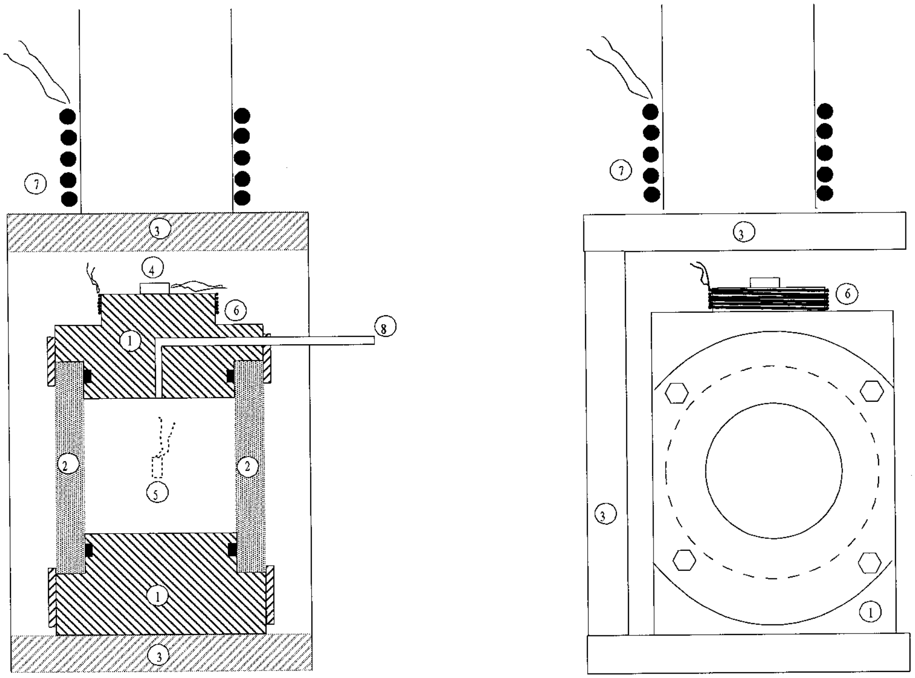

FIG. 1. General view of a closed cell. Gas is injected through the gas inlet (8). Heaters (6) and (7) control the thermal gradient and the cell temperature. Temperature measurements are performed with two silicon diodes (4) and (5). Two windows (2) allow the infrared beam to cross the cell.

$\sim$3800 to 11,500 cm^{-1}). This study contains the laboratory data used by Cruikshank *et al.* (1993) and Owen *et al.* (1993), but also new results obtained mainly using closed cryogenic cells. The data presented here are necessary to help interpret the current spectral observations of Triton and Pluto, and will continue to be of use as new measurements of these objects are made. In particular, it is necessary to understand better the origin of the shift of the CH_4 bands contained in astronomical spectra with respect to those of pure CH_4 ice measured in the laboratory. This

TABLE I
Main Physical Properties of the Pure Ices N_2, CH_4, C_2H_2, C_2H_6, CO, and CO_2

	Melting Point	**Phase Transit. Temperature**	**Crystal Group**	**Mol. / Unit Cell Site group**
N_2[1]	63.15 K	$T_{\alpha\text{-}\beta}$: 35.6 K	α phase : Pa3 (o-o) β phase : P63/mmc (o-d)	4 M/UC. ; Site S_6 2 M/U C. ; Site D_{3h}
CH_4[2]	90.4 K	$T_{II\text{-}I}$: 20.4 K	Phase II : Fm3c (o-p) Phase I : Fm3c (o-d)	8 M/UC ; 6 D_{2d} - 2 O_h 8 M/UC ; Site O_h
C_2H_4[3]	103.97 K	$T_{III\text{-}II}$ < 20 K $T_{II\text{-}I}$ ~ 50 K	Phase I : $P2_1/n$ (o-o)	2 M/UC ; Site C_i
C_2H_6[4]	89.28 K	$T_{II\text{-}I}$: 89 K	Phase I : disordered Phase II : $P2_1/n$ (o-o)	2 M/UC ; Site C_i
CO[5]	68.14 K	$T_{\alpha\text{-}\beta}$: 61.6 K	α phase : $P2_13$ (o-d) β phase : $P6_3/mmc$ (o-d)	4 M/UC ; Site S_6 2 M/UC ; Site D_{3h}
CO_2[6,7]	216.58 K	---	Pa3	4 M/UC ; Site S_6

Note. The highest-temperature crystal phase is by convention called I, and the others are numbered with decreasing temperatures; for N_2 and CO, the α phase is the coldest. The labels o–o, o–p, and o–d indicate orientationally ordered, partially ordered, and orientationally disordered, respectively. [1] Scott 1976; [2] Calvani *et al.* 1992; [3] Rytter and Gruen 1979; [4] Wisnosky *et al.* 1983a,b; [5] Löwen *et al.* 1990; [6] Löwen *et al.* 1989; [7] Falk 1987.

TABLE II
Main Spectroscopic Studies on the N_2, CH_4, C_2H_2, C_2H_6, CO, and CO_2 Molecules, as Pure Ices and Diluted in Matrices

	Sample and Spectral range	Measurement and/or Particular points
N_2	*Pure solid N_2* ; Fundamental region ~ 2327 cm^{-1} Löwen et al. (1990) Cardini et al. (1992) Scheidt (1993) Tryka et al. (1995)	Stretching mode at 2327 cm^{-1} induced by crystal defects or impurities in α-N_2 Fredin et al. (1974) Nelander (1976) Carr et al. (1980) Di Lella and Tevault (1986)
	Pure solid N_2 ; Overtone region ~ 4656 cm^{-1} Schmitt et al. (1990) Green et al. (1991) Grundy et al. (1993) Tryka et al. (1993) Legay and Legay-Sommaire (1996)	Origin of the infrared activity of the features Quirico et al. (1996)
CH_4	*Pure CH_4 ice* ; Mid-infrared Ewing (1964) Savoie and Fourier (1970) Chapados and Cabana (1972) Roux et al. (1980) Baran and Medina (1986) Baciocco et al. (1987)	Optical constants
	Pure CH_4 ice ; Range 500-9000 cm^{-1} Khare et al. (1990) Pearl et al. (1991)	Optical constants
	Pure CH_4 ice ; Range 4000-12000 cm^{-1} Calvani et al. (1992)	Band assignment
	Isolated molecule in matrices ; Mid-infrared Cabana et al. (1963) Chamberland et al. (1970) Nelander (1985) Llewellyn et al. (1986)	Specific study of the ν_3 and ν_4 bands ; Molecule-Matrix interactions
C_2H_4	*Pure C_2H_4 ice* ; Far-infrared Brith and Ron (1969) Schwartz et al. (1971)	
	Pure C_2H_4 ice ; Range 600-3500 cm^{-1} Brecher and Haldford (1961) Dows (1962)	Band assignment
	Isolated molecule in matrix ; Mid-infrared Collins et al. (1988)	

study can help us to derive new information about the physical state of CH_4, and recent progress on this subject will be presented in other papers (Quirico *et al.* in preparation, Douté *et al.* in preparation). Finally, we conclude the paper by exposing briefly the way these experimental results could be applied to the spectral analysis of Triton and Pluto spectra.

2. DESCRIPTION OF THE EXPERIMENTAL SETUP

Our experimental setup consists of a FTIR spectrometer (Nicolet 800) that records transmission spectra and a cryogenic system used to produce ice samples.

The cryogenic system consists of a high-vacuum optical cell with KBr windows at both optical ports, maintained

TABLE II—*Continued*

	Sample and Spectral range	Measurement and/or Particular points
C_2H_6	*Pure C_2H_6 ice* ; Mid-infrared Wisnosky et al. (1983-a) Tejada and Eggers (1976)	
	Pure C_2H_6 ice ; Near-infrared Pearl et al. (1991) Schmitt et al. (1992)	
CO	*Pure CO* ; Fundamental region Ewing and Pimentel (1961) Ewing (1962) Löwen et al. (1990)	
	Pure CO ; first overtone Fink et Sill (1982) Legay and Legay-Sommaire (1982)	Band assignment
	Pure CO ; second overtone Legay-Sommaire and Legay (1982)	
	Isolated molecule in matrix ; fundam. Leroi et al. (1964) Dubost and Abouaf-Marguin (1972) Dubost (1976) Dubost et al. (1982)	
CO_2	*Pure CO_2 ice* ; many studies Warren (1986) Löwen et al. (1989) Bini et al. (1993), and references therein	Optical constants (UV-FIR) Band assignment and solid state physics
	Pure CO_2 ice ; Near-infrared Hansen (1992)	Optical constants
	Isolated molecule in matrix ; mid-IR Irvine et al. (1982)	

under vacuum (less than 10^{-7} mbar), and placed in the sample compartment of the spectrometer. Inside this optical cell, a sample holder is fitted at the top of the cold finger of a closed-cycle He cryostat, with its temperature monitored using calibrated silicon diodes and a PID controller (Lake Shore DRC-93CA). Two types of sample holders and techniques can be used: (1) direct deposition on a single window (thin-film technique), and (2) crystal growth from the liquid phase in a closed cell.

2.1. Thin-Film Technique

In our system, thin films of ices are obtained from condensation of molecules on a cold MgF_2 or CsI window. The thickness of the sample is measured during deposition from the interference fringes of the transmitted and reflected beams of a He–Ne laser (beam incidence, ~45°). The optical quality of the film is evaluated by monitoring the intensity of the reflected laser beam, as well as the magnitude of the interference fringes. The crystallographic quality can be evaluated by means of specific absorption bands induced by crystal defects and, more generally, by the linewidth temperature dependence (Foggi and Schettino 1992).

The variable that seems to most affect the quality of the films as they are deposited is the condensation temperature, which should be greater than the diffusion temperature (Cardini *et al.* 1992); however, the deposition rate is also an important parameter. Very low deposition rates result in excellent-optical-quality films with thicknesses up to several hundred microns (deposition for about 200 hr at 3.5 μm/hr on a CsI window).

Thin-film technique presents two advantages. Experiments are quick and easy to perform, and films with good optical quality of a few microns and with well-known thicknesses can be obtained; however, several limitations have

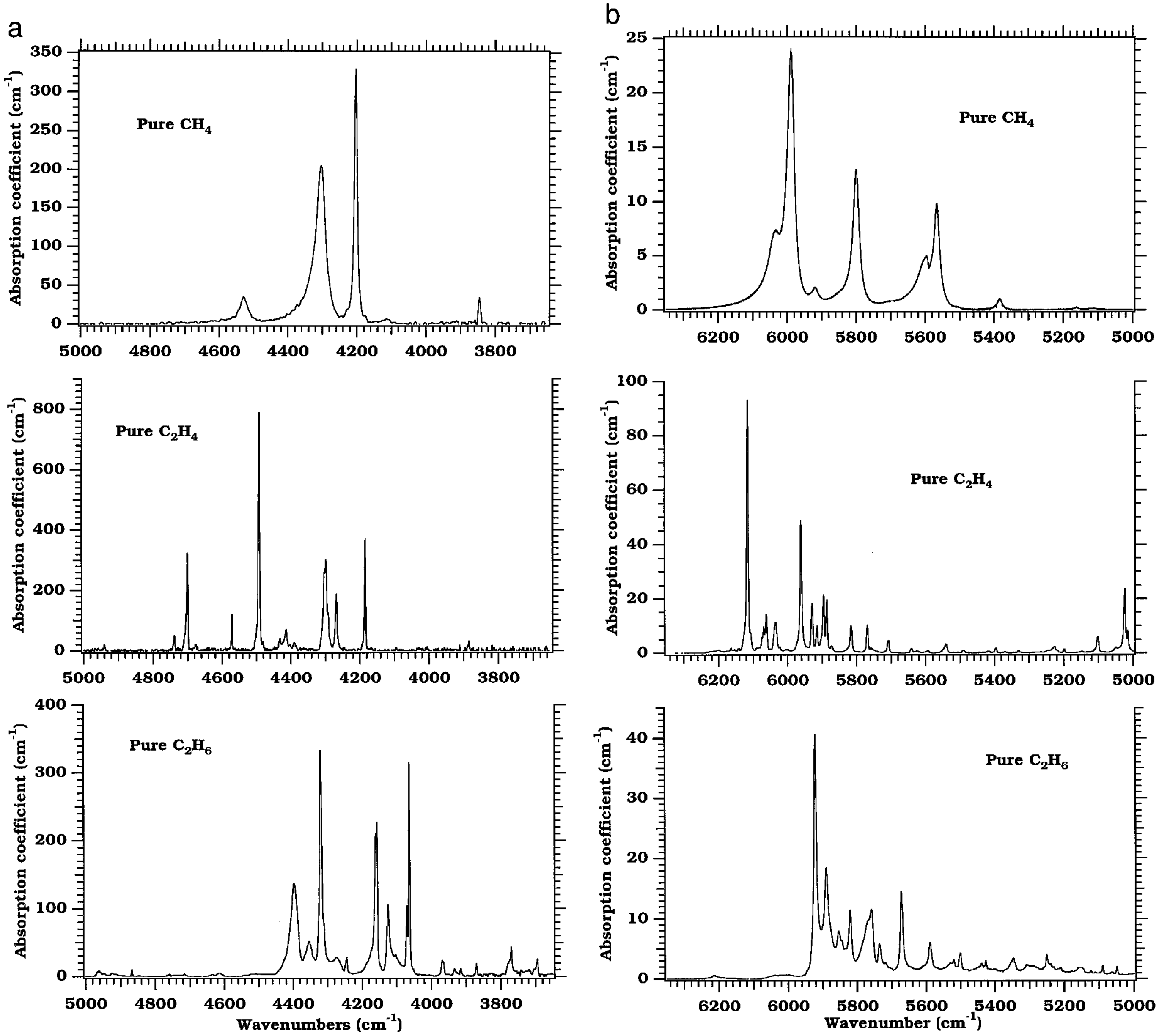

FIG. 2. Spectra of pure solid CH_4, C_2H_4, and C_2H_6. Experiments were performed with thin films condensed at 21 K with a spectral resolution of 2 cm^{-1}.

to be pointed out. Contamination of the sample (especially by H_2O and CO_2) is particularly strong for slow deposition rates. The range of temperature that can be investigated is restricted due to sample evaporation since the sample is in direct contact with the cell vacuum. Finally, a limited range of sample thicknesses can be prepared. During the growth of thicker films, it becomes progressively more difficult to measure the thickness accurately, because of the loss of He–Ne interference fringes. Finally, for the thickest films, poor crystal quality becomes a problem, preventing the infrared beam from going through the sample.

A particular limitation occurs for molecular mixtures. The absolute concentration in the film (with respect to the gas phase from which the film is formed) and the way the molecules are mixed are largely unknown. These are unknowns because, as will be discussed in Section 4, molecules may have different sticking coefficients at the condensation temperature, and the film is not formed at thermodynamical equilibrium. It is thus sensitive to experimental conditions, and furthermore, complex chemicophysical processes occur during growth (e.g., molecular diffusion on the film surface).

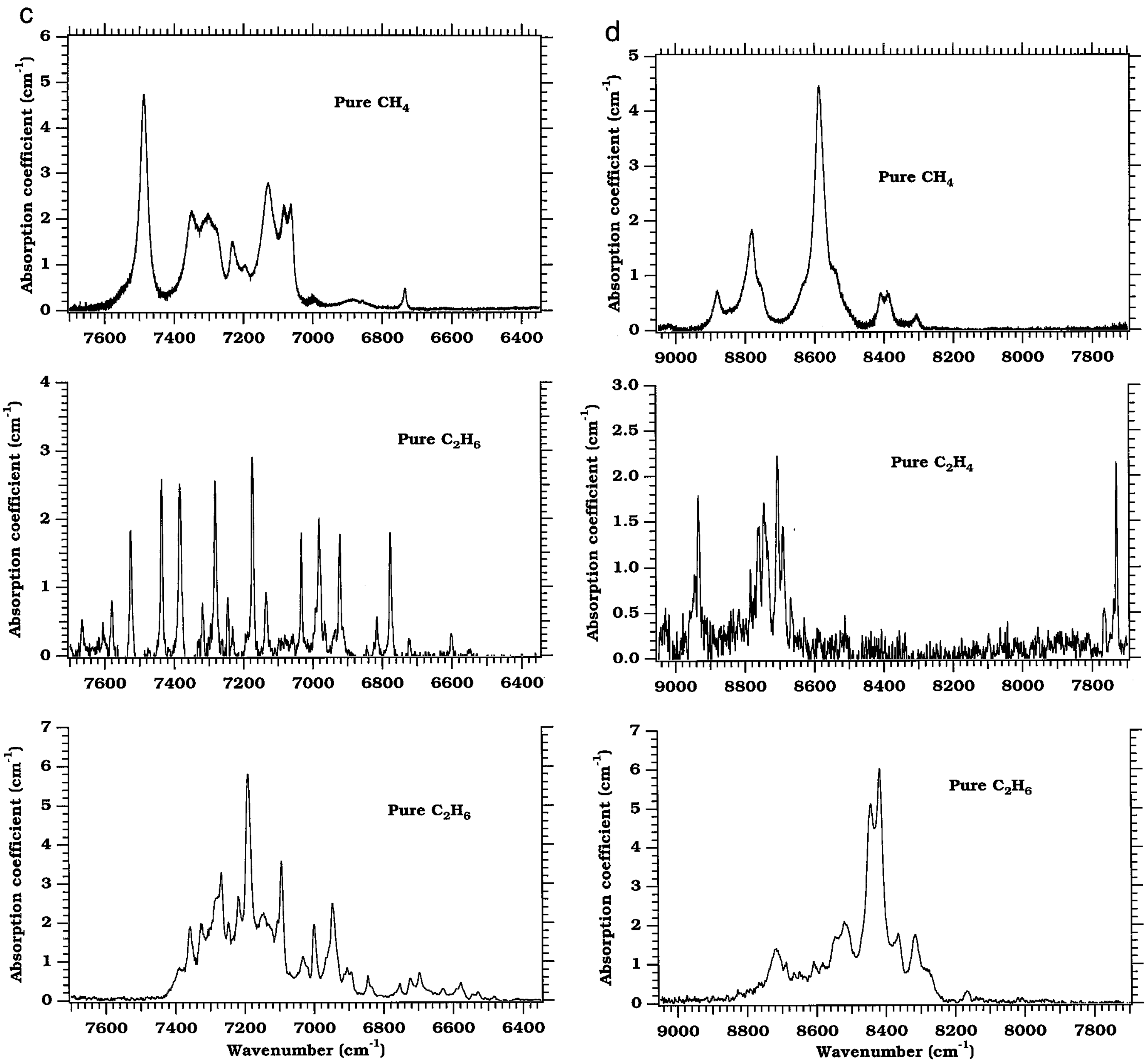

FIG. 2—*Continued*

2.2. Closed Cell Technique

This technique allows crystals to be grown from the liquid in a closed cryogenic cell. A schematic view is shown in Fig. 1. The cell (1) has two windows (2) sealed with indium gaskets, and is connected to the finger of the cryostat with a copper handle (3). The temperature at the top and at the middle of the cell are respectively measured with the silicon diodes (4) and (5) (at least one of them is calibrated ±0.05 K). Heater (7) heats the whole cell, whereas heater (6) establishes a vertical thermal gradient in the cell. The first heater is controlled by a PID controller; the second is connected to a stabilized power supply.

Crystals are grown as follows. The cell is cooled down to a temperature slightly greater than the melting point and the thermal gradient is established using heater (6). The cell is filled with gas (which condenses immediately to liquid) via the gas inlet (8). When the chamber is full of liquid, the cell is slowly cooled down via the temperature controller and heater (7). The crystal grows from the bottom to the top. The temperature is stabilized when a crystal

TABLE III
Absorption Bands of Pure Solid CH_4

Band frequency (cm^{-1})	Absorption coefficient (cm^{-1})	Vibration mode	Band frequency (cm^{-1})	Absorption coefficient (cm^{-1})	Vibration mode
3845.7	34	$3\nu_4$	6998.7	< 1	?
4116.1	7	$\nu_2+2\nu_4$	7063.6 7083.5	2 2	$2\nu_1+\nu_4$
4203.2	329	$\nu_1+\nu_4$			
4303.6	205	$\nu_3+\nu_4$	7129.3	3	$\nu_1+\nu_3+\nu_4$
			7195.9	1	$\nu_1+2\nu_2+\nu_4$
4529.6	35	$\nu_2+\nu_3$	-------- 7232.4	 1.5	
-------- 5161.6	 1	$4\nu_4$	-------- 7302.4	 2	$2\nu_3+\nu_4$
5383.2		$\nu_1+2\nu_4$			
5565.8 5595.2	10 5	$\nu_3+2\nu_4$	--------		$[\nu_3]+[\nu_3]+[\nu_4]$
			7350.2	2	$\nu_1+\nu_2+\nu_3$
--------		$2\nu_2+2\nu_4$	7487.1 --------	4.5	$\nu_2+2\nu_3$
--------		$\nu_1+\nu_2+\nu_4$			
5799.9	13	$\nu_2+\nu_3+\nu_4$	8306.2	< 1	$\nu_1+\nu_2+3\nu_4$
--------		$3\nu_2+\nu_4$	8388.0	< 1	$2\nu_1+2\nu_4$
5919.3	2	$\nu_1+\nu_3$ (?)	--------		$[\nu_1]+[\nu_1]+[2\nu_4]$
5989.2	24	$2\nu_3$	8408.9	< 1	$[\nu_1]+[\nu_1]+[\nu_4]+[\nu_4]$
6033.4	7	$[\nu_3]+[\nu_3]$ (?) $2\nu_2+\nu_3$ (*)	~ 8541	1	$\nu_1+\nu_3+2\nu_4$
6734.2	< 1	$\nu_1+3\nu_4$	8587.1	4.5	$2\nu_3+2\nu_4$
6857.6 ~6883	< 1 < 1	$\nu_3+3\nu_4$	~ 8756	< 1	$2\nu_1+\nu_3$
			8781.4	1.5	$\nu_2+2\nu_3+\nu_4$
			8881.0	1	$\nu_1+2\nu_3$

Note. The spectral assignment is due to Calvani *et al.* (1992). Suspect assignments are accompanied by a question mark, and an asterisk indicates a new assignment we propose (see text). Modes indicated in square brackets correspond to multivibron transitions. The dash sign means that a band is not observed.

is obtained, and it is annealed for about 12 hr. Finally, the thermal gradient is set to zero and the study can begin. As will be seen in the following section, we had to operate slightly differently with the first closed cell we built (stainless-steel cell), because of its poor thermal performance, but it should be stressed that this is a special case.

We built three different closed cells. The first stainless-steel cell with MgF_2 windows allowed us to grow 1-cm-thick samples and to collect a large part of the data contained in this paper; however, this cell was not optimized. Temperature control was difficult (high thermal inertia), sample quality was in some cases insufficient, and only one thickness (1 cm) was available. Thus, we designed and built a new cell with the help of Roberto Bini (Laboratorio di Spettroscopia Molecolare, Florence, Italy), which provided very good results for sample thicknesses equal to or smaller than 1 mm and correct results for thicknesses ranging from 1 to 8 mm (cell is described in detail in Bini *et al.* 1992). As thick samples are of great interest for planetological studies, we finally built a third cell especially designed for 1-cm-thick samples. It is a brass cell with CaF_2 windows and with a chamber shape optimized to prevent crystal damage on cooling (the surface/volume ratio of the chamber has been increased as much as possible to limit differential contraction of the sample on cooling). At present, we use the last two cells exclusively.

TABLE IV
Absorption Bands of Pure Solid C_2H_4

Wavenumber (cm^{-1})	Absorption coefficient (cm^{-1})	Wavenumber (cm^{-1})	Absorption coefficient (cm^{-1})
3679.5	2	4677.6	23
3684.8	2	4701.5	324
3693.1	2	4738.7	51
3705.9	3.5	4941.3	15
3759.1	< 2	4955.4	7
3796.0	< 2	5015.2	8
3815.7	22	5023.2	23
3841.6	< 2	5049.3	2
3865.1	3.5	5100.0	6
3876.3	< 2	5199.5	< 2
3884.8	35	5225.4	2
3911.8	11	5331.9	< 2
3924.5	2	5396.8	< 2
3947.6	6	5488.1	< 2
3980.0	2	5540.6	3.5
4006.0	7	5639.9	< 2
4027.2	7	5643.4	< 2
4099.4	4.5	5706.9	4.5
4118.7	2	5768.6	9
4168.6	8	5816.4	10
4185.0	370	5873.5	2
4245.6	9	5887.0	20
4268.7	186	5896.1	21
4292.8	122	5914.8	9
4299.3	301	5929.1	18
4303.4	258	5962.1	48
4340.7	3.5	6035.2	11
4368.5	3.5	6062.6	14
4391.1	33	6070.3	9
4414.8	71	6116.6	92
4433.1	40	~6777.5	< 2
4482.7	27	~6921.3	< 2
4493.0	787	~6981.9	< 2
4524.3	2	~7033	< 2
4543.6	2	~7175.5	2
4572.2	117	~7282.5	2
4590.4	4.5	~7385	2
4616.6	6	~7437.5	2
4649.2	2	~7527	< 2
4658.3	3.5	~7730	< 2

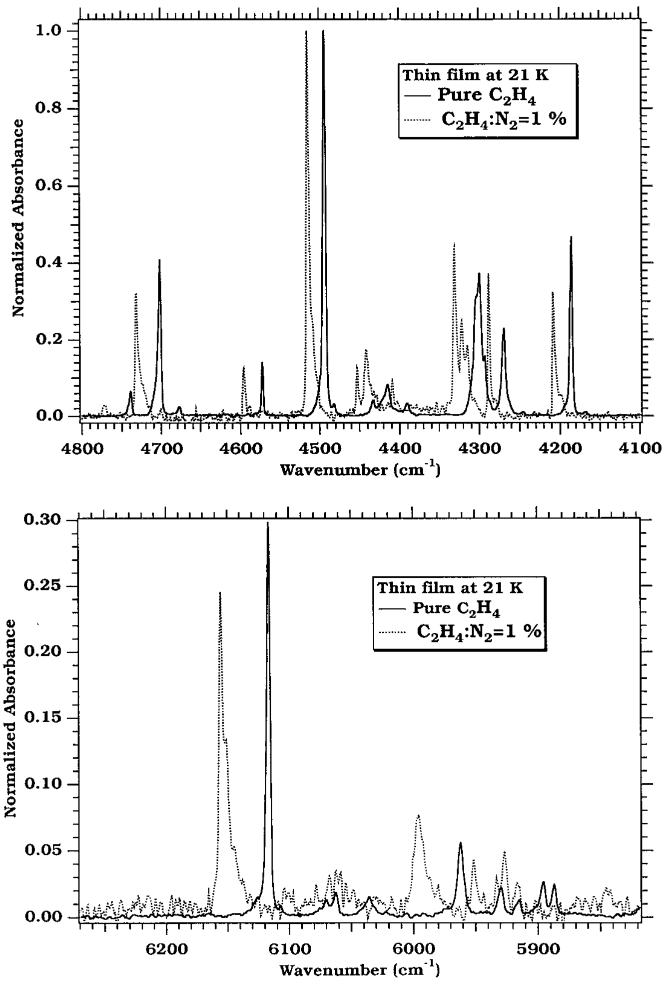

FIG. 3. Absorbance spectrum of a $C_2H_4:N_2$ mixture with 1% C_2H_4 compared with the spectrum of pure solid C_2H_4. Both spectra were obtained from thin films condensed and studied at 21 K. For each spectrum, the peak absorbance of the strongest band near 4500 cm^{-1} has been normalized to 1, and this normalization is used in both panels. Absorbance is defined as $\log(I_0/I)$, where I/I_0 is the fraction by which passing through the sample diminishes the intensity of the infrared spectrometer beam.

The closed cell technique has several decisive advantages over thin-film techniques. Thick samples (up to 1 cm) with good optical and crystal qualities can be obtained and these qualities can be maintained during the experiment; the thickness can be accurately measured, and impurities are considerably reduced relative to thin films. In addition, crystal growth occurs under thermodynamical equilibrium, and experiments are perfectly reproducible (this thermal gradient is measured on moving the infrared spot on the sample). Some disadvantages have to be pointed out, however. In the case of molecular mixtures, a vertical concentration gradient is generally observed, and the absolute concentration cannot be accurately measured. It is also not possible to form phases outside the thermodynamical equilibrium (e.g., to obtain amorphous solids). Nor is it possible to obtain a thickness smaller than ~10 μm, and the technique is difficult and time consuming. Some of these last points are considered in detail in Section 4.

Nevertheless, these limitations are more than compensated for by the strong advantages. The closed cell appears,

TABLE V

Frequencies of Pure Solid C_2H_4 at 21 K and of C_2H_4 Molecules Trapped in a Nitrogen Matrix at 21 K ($C_2H_4:N_2 = 1:100$) and Frequency Shift between Identical Vibration Modes

WAVENUMBER (cm^{-1})		
Pure C_2H_4	Diluted 1%	$\nu_{dil}-\nu_{pure}$ (cm^{-1})
—	~4198	—
4185.0	4207.8	22.6
—	~4280	—
4268.7	4287.9	18.9
4292.8	4314.6	21.6
4299.3	4321.8	22.4
4303.4	4330.7	27.2
4391.1	4409.0	18.4
4414.8	4441.5	26.7
4433.1	4452.7	19.8
4493.0	4514.6	21.4
4572.2	4595.8	23.5
4701.5	4731.9	30.3
4738.7	4771.5	32.6

Note. Frequencies joined by a bracket correspond to different sublevels of a split band. Bands not observed are marked with dashes.

in many cases, to be the preferable technique for planetological studies.

3. SPECTRAL PROPERTIES OF MOLECULES DILUTED IN N_2 AND AS PURE ICES

In this section, we present experimental spectra of the pure ices CH_4, C_2H_4, C_2H_6, CO, and CO_2 and of these molecules (except CH_4, see Section 4) diluted in solid nitrogen. The spectral range investigated extends from ~3600 to ~10,000 cm^{-1} (1–2.7 μm), and all these spectra have been recorded under similar experimental conditions (except CH_4, see Section 3.1): from thin films condensed and studied at ~21 K, with a spectral resolution of 2 cm^{-1}. In the specific cases of pure CO and CO_2, quick additional experiments with the closed cell were performed with a spectral resolution of 1 cm^{-1}. Gases used were supplied by the Air Liquide Corporation (stated purity: 99.9999% for N_2 and 99.995% for other molecules).

For each of these molecules as pure ices, and in addition for pure N_2 ice, we indicate in Table I the most useful physical parameters (melting point, crystal phases, etc.). Table II lists the main papers dealing with spectroscopic measurements on these molecules as pure ices and diluted in matrices.

3.1. Solid Methane

Our measurements are shown in Fig. 2 and Table III. They have been obtained with thin films formed on a CsI window at 30 K and measured at 36 K and with samples grown in the copper closed cell for a 1-mm thickness. The maximum relative uncertainty on the absorption coefficients is estimated to be 10%.

Our results are in general agreement with those of Calvani *et al.* (1992) performed at 27 K; however, slight differences are observed between the two data sets: (1) We do not observe the second component of the $\nu_3 + \nu_4$ mode at 4285 cm^{-1}. (2) We measured a band at 6998.7 cm^{-1} they did not observe. (3) The $2\nu_3$ overtone is found at 5989.2 cm^{-1}, against 6010 cm^{-1} [but this is probably due to a typographical error (Calvani, personal communication)]. We also observed the splitting of the $2\nu_1 + \nu_4$ mode, as well as the $\nu_1 + \nu_2 + \nu_3$ vibration mode, at 7350.2 cm^{-1}, which is observed only in phase II by Calvani *et al.* (1992). A detailed study of the optical constants of pure CH_4 in the visible and near-infrared range as a function of temperature will be published elsewhere (Grundy *et al.* in preparation).

In addition to these measurements, we considered the question of band assignments on the basis on calculations performed for the isolated CH_4 molecule (Hilico *et al.* 1994, 1995) and also some results obtained for the CH_4 molecule isolated in N_2 (see Section 4). We generally agree with the assignments of Calvani *et al.* (1992), except for the bands peaking at 5919 and 5989 cm^{-1} in our measurements and assigned by Calvani *et al.* (1992) to respectively the $\nu_1 + \nu_3$ vibration mode and to the $[\nu_3] + [\nu_3]$ multivibron transition [also called the two-phonon continuum (see Quirico *et al.* 1996)].

We did not observe the band at 5919 cm^{-1} for the CH_4 molecule isolated in a N_2 matrix. In addition, calculations on the isolated molecule indicate that this vibration is in strong interaction with other ones and would peak at 5851 cm^{-1} (Hilico *et al.* 1994, 1995). Such a frequency is shifted with respect to 5919 cm^{-1}, whereas the shift between pure solid and isolated state does not exceed 20 cm^{-1} for the other bands in this spectral region. This assignment should thus not be considered definitive.

We observed the band at 5989 cm^{-1} for the CH_4 molecule isolated in solid N_2 as a broadband at 30 K and above (Fig. 10a) and as two components peaking at 6066.5 and 6056 cm^{-1} at 17 K. According to the Calvani *et al.* (1992) assignment, however, this band should not appear for matrix-isolated CH_4. Thus, a multivibron transition (here $[\nu_3] + [\nu_3]$) involves vibron propagation which does not exist for the isolated state in matrix, but only for pure ice (Quirico *et al.* 1996). On the other hand, theoretical calculations indicate two components of the $2\nu_2 + \nu_3$ vibration mode peaking at 6053.5 and 6046.5 cm^{-1} (Hilico *et al.* 1994, 1995).

TABLE VI
Absorption Bands of Pure Solid C_2H_6

Wavenumber (cm^{-1})	Absorption coefficient (cm^{-1})	Wavenumber (cm^{-1})	Absorption coefficient (cm^{-1})	Wavenumber (cm^{-1})	Absorption coefficient (cm^{-1})
3694.2	25	4925.3	4.5	5921.8	41
3768.7	41	4947.1	4.5	6213.9	< 2
3869.8	18	4950.8	4.5	6576.2	< 2
3914.6	11	4963.2	8	6628.1	< 2
3932.1	11	5047.4	2	6696.9	< 2
3950.5	2	5061.0	< 2	6723.6	< 2
⌈3965.4	21	5087.7	2	6753.8	< 2
⌊3968.2	23	5094.5	< 2	6843.7	< 2
⌈4063.2	315	5122.1	< 2	6903.9	< 2
|4069.5	103	5152.8	2	6946.0	2
⌊4072.3	60	5178.8	< 2	6998.5	< 2
4124.9	103	5210.6	2	7032.8	< 2
⌈4157.3	228	5230.6	2	7093.2	3.5
⌊4160.6	209	5238.7	2	7105.1	< 2
4245.5	28	5248.2	4.5	7145.0	2
4274.8	28	5307.6	2	7187.3	6
4320.7	333	5346.3	3.5	7215.7	2
⌈4352.1	53	5399.1	< 2	7248.0	< 2
⌊4353.5	53	5425.3	3.5	7266.9	3.5
4398.0	138	5437.5	2	7325.0	< 2
4615.0	6	5502.9	4.5	7327.3	< 2
4636.9	3.5	5517.8	3.5	7356.5	< 2
4680.4	< 2	5528.9	2	~8324	< 2
4715.6	4.5	5587.7	6	~8315	< 2
4741.1	2	5670.1	15	~8363	< 2
4759.0	3.5	5734.8	6	⌈~8414	6
4764.3	2	5757.9	11	⌊~8436	6
4847.6	< 2	5819.8	11	~8519	< 2
4867.4	9	⌈5844.4	7	~8690	< 2
4879.0	< 2	⌊5853.6	8	~8712	< 2
4887.7	< 2	5889.0	18		

Thus, with respect to these points, we think it more reasonable to assign this band to these two vibrational sublevels of the $2\nu_2 + \nu_3$ mode.

3.2. C_2H_4 Diluted in Solid N_2 and as Pure Ice

The spectra of pure C_2H_4 at 21 K are shown in Figure 2. The absorption coefficients and the positions of the bands are given in Table IV. The bands at 4701.6, 4493.0, 4414.8, and 4185.2 cm^{-1} are asymmetric with a high frequency shoulder. The spectral region above 6400 cm^{-1} is noisy; thus only accurate information about peak positions can be extracted. We point out that we observed slight spectral changes with increasing thickness during deposition, such as a slight shift that did not exceed 1 cm^{-1}.

The effects of dilution in α-nitrogen (1% C_2H_4) at 21 K were observed in the region 4800–4100 cm^{-1}. The spectra are displayed in Fig. 3 and Table V [absorbance is defined as $\log(I_0/I)$, where I_0 is the intensity of the infrared beam before passing through the sample, and I is the intensity afterward; for each spectrum, the peak absorbance of the strongest band has been normalized to 1]. First, we observed a general shift of the bands ranging between +18 and +33 cm^{-1} compared with the positions found for pure C_2H_4 ($\Delta\nu = \nu_{\text{diluted}} - \nu_{\text{pure}}$). Second, some particular effects modified each band of the spectra: the shoulder on the side of several asymmetric bands changed, and the unresolved group of bands at 4292.8, 4299.3, and 4303.4 cm^{-1} split into several components. The relative peak intensities of the bands were also slightly modified.

3.3. C_2H_6 Diluted in Solid N_2 and as Pure Ice

The spectra of pure C_2H_6 at 21 K are shown in Figure 2. The absorption coefficients and the positions of the bands are given in Table VI. We also point out that some split bands (~3966, ~4158, and ~4352 cm^{-1}) were found to be very sensitive to the thickness. During deposition, only one of the two components was observed. The second appeared on increasing thickness. For even thicker samples, only the second component remained.

TABLE VII

Frequencies of Pure Solid C_2H_6 at 21 K and of C_2H_6 Molecules Trapped in a Nitrogen Matrix at 21 K ($C_2H_6:N_2 = 1:100$) and Frequency Shift between Identical Vibration Modes

WAVENUMBER (cm^{-1})		
Pure C_2H_6	Diluted 1%	$\nu_{dil}-\nu_{pure}$ (cm^{-1})
4063.2 4069.5	——— 4083.1	—— 13.6
———	4090.0	——
4124.9	4141.8	16.9
4157.3 4160.6	4180.5 ———	23.2 ——
———	4200.0	——
4245.5	4264.6	19.1
4274.8	4283.9	9.5
4320.7	4338.9	18.2
4353.5	4376.2	22.7
4398.0 ———	4407.6 4425.3	~18.5 ——
5670.1	5697.1	
5734.8	~5761	~26.2
5757.9	5791	33.1
5819.8	5845.9	26.1
5844.4 5853.6	~5868 ———	~18 ——
5889.0	5913.8	24.8
5921.8	5946.1	24.3

Note. Frequencies joined by a bracket correspond to different sublevels of a split band. Bands not observed are marked with dashes.

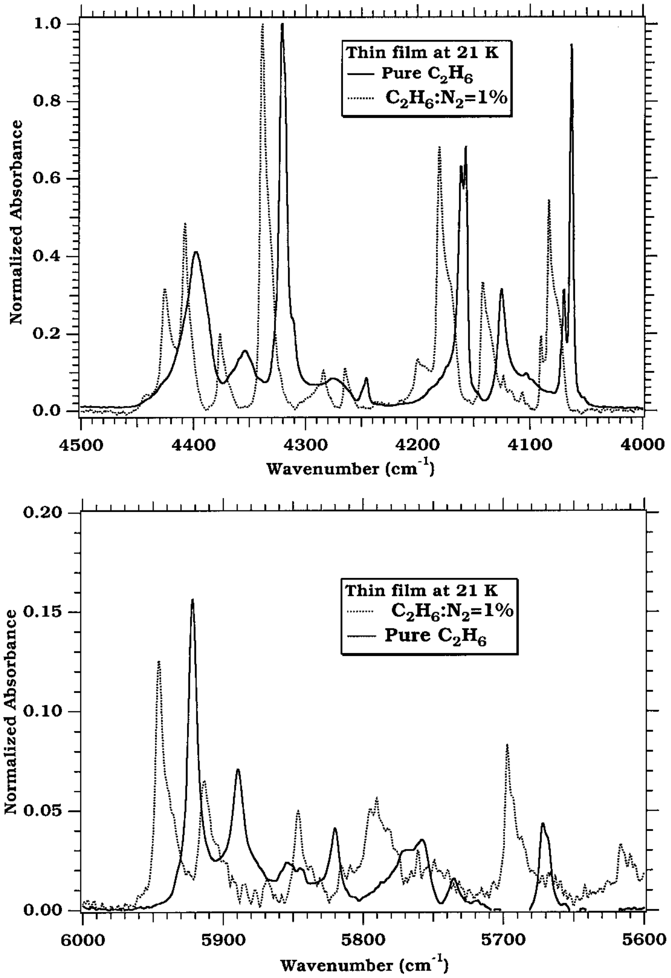

FIG. 4. Absorbance spectrum of a $C_2H_6:N_2$ mixture with 1% C_2H_6 compared with the spectrum of pure solid C_2H_6. Both spectra are obtained from thin films condensed and studied at 21 K. Normalization as in Fig. 3.

The effects of dilution in α-nitrogen (1% C_2H_6) at 21 K were observed in the regions 4500–4000 and 6000–5600 cm^{-1} (Table VII, Fig. 4). As for C_2H_4, we observed general shifts ranging from 10 to 23 cm^{-1} for the region 4500–4000 cm^{-1} and from 18 to 33 cm^{-1} for the region 6000–5600 cm^{-1}. Particular effects on each band appear more pronounced than in the case of C_2H_4: (1) the broadband at 4398 cm^{-1} splits into two components at 4407.6 and 4425.3 cm^{-1}; (2) the two bands at 4157.3 and 4160.6 cm^{-1} merge into an asymmetric band with unresolved components; (3) similar behavior occurs for the bands at 4063.2 and 4069.5 cm^{-1} with strong changes in relative intensities; (4) a new band appears at 4090.0 cm^{-1}.

3.4. *CO Diluted in Solid N_2 and as Pure Ice*

The bands measured at 21 K in the first and second overtone regions of CO are assigned using the work of Legay and Legay-Sommaire (1982) (Fig. 5, Table VIII). The spectrum of 1% CO diluted in α-nitrogen at 21 K shows a slight shift ($\sim$+1 cm^{-1}) of the peak frequency of the first overtone and a large decrease in the bandwidth: the FWHM is 2.6 cm^{-1} for solid CO and is reduced to 1 cm^{-1} for 1% diluted CO. A complete study of CO diluted in solid N_2 is presented in Quirico and Schmitt (1996).

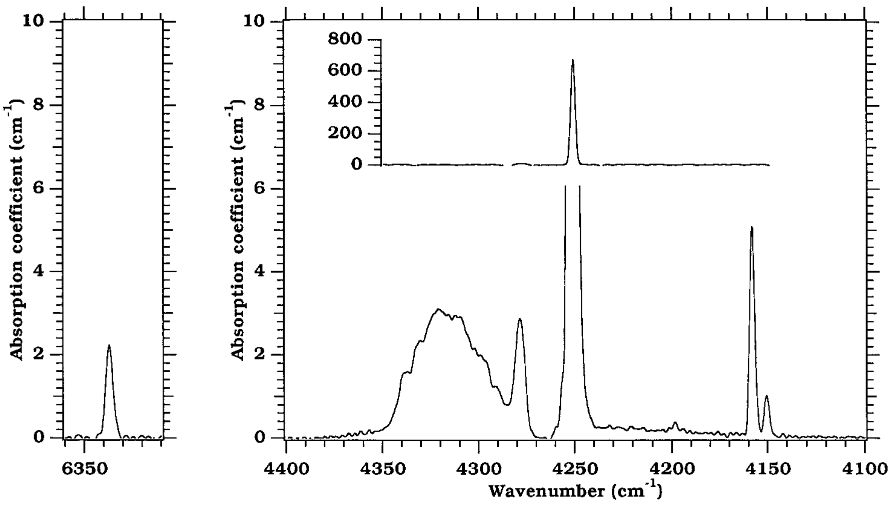

FIG. 5. Absorbance spectrum of pure solid CO in the first and second overtone regions. The full-scale plot inside the figure shows the main 4250 cm^{-1} band, measured on a thinner sample.

3.5. CO_2 Diluted in Solid N_2 and as Pure Ice

The thin films of pure CO_2 condensed at 21 K were not amorphous as might have been expected (Falk 1987). We assigned the strongest vibrational bands observed in the spectra of pure solid CO_2 (Fig. 6, Table IX), using the infrared selection rules from Herzberg (1948). Using measurements performed at 180 K on a sample grown in the closed cell, we observed that the absorption bands were slightly shifted toward shorter wavenumbers (~4 cm^{-1}) with respect to the values found for thin CO_2 films at 21 K.

The effect of dilution of CO_2 (0.25%) in the α phase of solid nitrogen was studied using thin-film experiments (Table X). On dilution, shifts toward higher frequency were observed: +4.5, +2.3, and +11 cm^{-1} for the $2\nu_1 + \nu_3$, $\nu_1 + 2\nu_2 + \nu_3$, and $4\nu_2 + \nu_3$ bands, respectively. We also observed a new and weak band at 4676.8 cm^{-1} which does not appear in the spectra of pure CO_2. This band could be the infrared forbidden $2\nu_3$ transition, activated in the anisotropic nitrogen matrix. The quality of our spectra did not allow us to compare the width and shape of the bands.

TABLE VIII
Absorption Bands of Solid CO

Wavenumber (cm^{-1})	Absorption coefficient (cm^{-1})	Vibration mode
4150.5	1	$^{12}C^{18}O$ / 2ν
4158.0	5	$^{13}C^{16}O$ / 2ν
4198.2	0.2	$^{12}C^{17}O$ / 2ν
4250.9	672	$^{12}C^{16}O$ / 2ν
4278.3	3	[ν]+[ν]
~4314	~ 2	phonon sideband
6337	2.5	3ν

Note. The spectral assignment is due to Legay and Legay-Sommaire (1982) and Legay-Sommaire and Legay (1982). Square brackets are indicative of multivibron transitions.

4. EXPERIMENTAL STUDY OF CH_4 DILUTED IN SOLID N_2

We present now a systematic study of CH_4 diluted in solid N_2 as a function of concentration and temperature. This study was performed first on thin films for different CH_4 concentrations and for a constant temperature of 21 K (Section 4.1), and then on samples grown in closed cells, which allowed us to perform measurements in an extended temperature range (15–63.15 K) and also for different CH_4 concentrations (Section 4.2). The results obtained are independently discussed, and finally compared with each other (Section 4.3).

The thin-film measurements are those that were used in Cruikshank *et al.* (1993) and Owen *et al.* (1993), and there are at least two reasons to present them here: (1) it gives detailed information about the spectral analyses conducted by these authors; (2) their comparisons with the measurements obtained in a closed cell give important results from a methodological point of view.

4.1. Thin-Film Experiments

Several thin-film experiments were performed, which allowed us to observe the strongest CH_4 bands $\nu_1 + \nu_4$ and

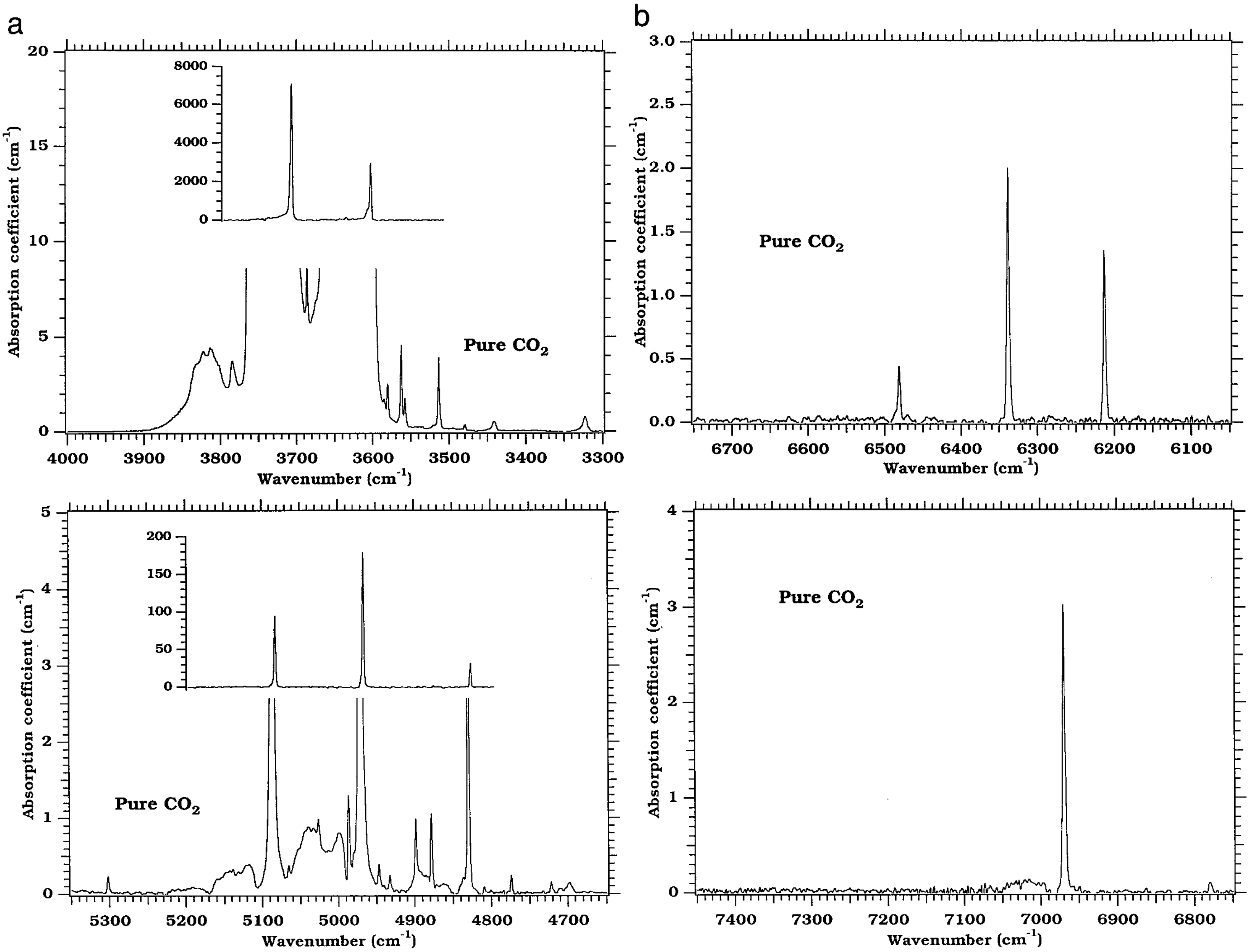

FIG. 6. (a) Normalized absorbance spectrum of pure solid CO$_2$. The full-scale plots inside the figure show the main bands, measured on thinner samples. The same normalization applies to both panels. (b) Same as (a), without the inset full-scale plots.

$\nu_3 + \nu_4$ around 4200 and 4300 cm^{-1}. We performed three experiments with CH$_4$ concentrations of 0.25, 1, and 10% (nominal concentration of the gaseous mixture from which the film is formed), for thin films formed under quite similar experimental conditions (condensed on a MgF$_2$ window at about 21 K with deposition rates in the range 0.05–0.5 μm min^{-1}).

In addition to these three experiments, we studied two other samples with a CH$_4$ concentration of 1%, but under different experimental conditions (condensation temperature, deposition rate), to test the experimental reproducibility.

Experimental results. For the three experiments at 0.25, 1, and 10% CH$_4$, the main effects of dilution of CH$_4$ in nitrogen are a general shift of the bands compared with their positions for pure CH$_4$ (Table XI) and some changes in band profiles and peak intensities (Fig. 7).

At 10% concentration (Fig. 7), the $\nu_1 + \nu_4$ and the $\nu_3 + \nu_4$ bands are slightly shifted (respectively +3.4 cm^{-1} and +1.9 cm^{-1}), compared with the values found for pure methane at the same temperature. At the same temperature, the relative peak intensities are changed, and both bands are slightly broadened. With 1% CH$_4$ in N$_2$ (Fig. 7), the $\nu_1 + \nu_4$ band is broadened and shifted to about 4212.5 cm^{-1} (shift: +~9.5 cm^{-1}), compared with pure methane. This band seems to be the sum of several very closely spaced components. The $\nu_3 + \nu_4$ band is split into two bands at 4326.2 cm^{-1} (shift: +23.2 cm^{-1}) and 4307.8 cm^{-1} (shift: +4.8 cm^{-1}), and a shoulder is observed at ~4340 cm^{-1}. At a CH$_4$ concentration of 0.25% (Fig. 3), the $\nu_1 + \nu_4$ band presents only one narrow component at 4217.7 cm^{-1} (shift: +14.5 cm^{-1}). The $\nu_3 + \nu_4$ band presents one main component at 4326.6 cm^{-1} (shift: +23.6 cm^{-1}) and three additional components at 4340, 4315, and 4309 cm^{-1}.

TABLE IX
Absorption Bands of Solid CO_2

Wavenumber (cm^{-1})	Absorption coefficient (cm^{-1})	Vibration mode
3599.1	2957	$^{(f.r\ 1)}2\nu_2+\nu_3$
3632.4	172	
3667.3	60	
3686.4	8.5	
3708.0	7056	$^{(f.r\ 1)}\nu_1+\nu_3$
3784.0	3.5	
3812.5	4.5	
3822.4	4	
4632.4	< 1	
4636.9	<1	
4697.6	< 1	
4721.5	< 1	
4773.7	< 1	
4830.5	31	$^{(f.r\ 2)}4\nu_2+\nu_3$
4878.5	1	
4898.7	1	
4933.0	< 1	
4947.2	< 1	
4971.2	178	$^{(f.r\ 2)}\nu_1+2\nu_2+\nu_3$
4986.9	1.5	
4998.7	< 1	
5026.8	< 1	
5033.4	< 1	
5039.8	< 1	
5065.6	< 1	
5086.6	94	$^{(f.r\ 2)}2\nu_1+\nu_3$
5302.4	< 1	
6042.1	< 1	$^{(f.r\ 3)}6\nu_2+\nu_3$
6213.1	1.5	$^{(f.r\ 3)}\nu_1+4\nu_2+\nu_3$
6339.1	2	$^{(f.r\ 3)}2\nu_1+2\nu_2+\nu_3$
6481.5	< 1	$^{(f.r\ 3)}3\nu_1+\nu_3$
6970.1	3	$3\nu_3$

Note. The third column indicates the assignment we performed using the assignment of the vibration modes of the isolated molecule (Herzberg 1948). Bands in Fermi resonance are indicated by "f.r", and the associated number distinguishes the different groups of bands that are interacting with one another.

TABLE X
Frequencies of CO_2 Molecules Trapped in a Nitrogen Matrix at 21 K ($CO_2:N_2$ = 0.25 : 99.75) and of Pure Solid CO_2 and Frequency Shift between Identical Vibration Modes

Diluted 0.25%	Pure CO_2	$\nu_{dil}-\nu_{pure}$ (cm^{-1})	Vibration Mode
3606.1 3609.2	3599.1	7	$2\nu_2+\nu_3$
3710.5 3713.5	3708.0	2.5	$\nu_1+\nu_3$
4841.5	4830.5	11	$4\nu_2+\nu_3$
4973.8	4971.5	2.6	$\nu_1+2\nu_2+\nu_3$
5091.1	5086.6	4.5	$2\nu_1+\nu_3$

We also observed the ν_3 fundamental band (Fig. 8). At 0.25% CH_4 in N_2, this band is asymmetric and presents four blended components. The peak frequency of the stronger one is 3030 cm^{-1}, and the three others with decreasing intensity are shifted toward lower frequencies. At 1% concentration, the ν_3 fundamental appears as a main band at 3015 cm^{-1} with a shoulder on the high-frequency wing, possibly with two components.

For the three experiments at the same CH_4 concentration of 1%, we observed that the spectra are dramatically sensitive to experimental conditions (Fig. 9). The spectral profiles of the $\nu_1 + \nu_4$ and $\nu_3 + \nu_4$ bands, as well as the positions of their components, are different from one experiment to the other. The B experiment exhibits the $\nu_1 + \nu_4$ band split in two components, the lower-frequency one having a frequency close to that of pure CH_4 ice, whereas a broadband is observed in the A experiment (previously described in detail); the $\nu_3 + \nu_4$ band has two components, but with respect to experiment A, the low-frequency component has a frequency close to that of pure CH_4 ice. Finally, experiment C looks different from experiment B on the basis of the intensity of the high-frequency component, which is weaker than for experiment B.

Discussion. We now attempt to explain the concentration dependence of spectra of the three samples with 0.25, 1, and 10% CH_4 and also the sensitivity of the spectra to experimental conditions of the spectra for the given concentration of 1%.

According to the classic treatment of molecules trapped in matrices, the guest CH_4 molecules can exist as isolated molecules or as clusters of various sizes in the nitrogen matrix (dimer, trimer, etc.). In the specific case of an isolated CH_4 molecule (i.e., which has only N_2 molecules as

TABLE XI

Peak Frequencies of the $\nu_1 + \nu_4$ and $\nu_3 + \nu_4$ Bands of Methane for Pure Solid and for Methane Diluted in a Nitrogen Matrix with $CH_4:N_2$ = 10:90, 1:99, and 0.25:99.75

Pure CH_4 (21 K)	dil - 10 % (21 K)	Shift (cm^{-1})	dil - 1 % (21 K)	Shift (cm^{-1})	dil-0.25 % (21 K)	Shift (cm^{-1})	Mode
4203.2	4206.6	+ 3.4	~4212.5	+ ~9.5	4217.7	+ 14.5	ν_1+ν_4
4303.0	4304.9	+ 1.9	4326.2 4307.8	+ 23.2 + 4.8	4326.6 4340 4315 4309	+ 23.6	ν_3+ν_4

Note. Samples are thin films condensed and studied at about 21 K.

first neighbors), the motion of the molecule in the α phase of the nitrogen matrix is a slightly hindered rotation (Nelander 1985), and we can reasonably suspect it is the same in the β phase of solid nitrogen, because this phase is orientationally disordered (the CH_4 bands in this phase looks like those observed in the liquid). Thus, the CH_4 bands for a monomer are in fact a rovibrational fine structure; however, for a cluster, the different CH_4 molecules interact with each other. The molecular rotational motion is perturbed or no longer exists, and the profile of a band can be strongly modified with respect to that of the isolated molecule (monomer). Consequently, a CH_4 absorption band can be the sum of the different bands corresponding to the monomer and the various clusters all present in the sample, and the effect of CH_4 concentration on the shape and peak frequency of the bands can be partly explained in terms of the statistical distribution of cluster sizes.

In the case of thin films with 10, 1, and 0.25% methane in solid nitrogen at 21 K, changes in the cluster populations can account for the changing shape of the $\nu_1 + \nu_4$ and $\nu_3 + \nu_4$ bands. With 10% CH_4 in N_2, the solid is probably

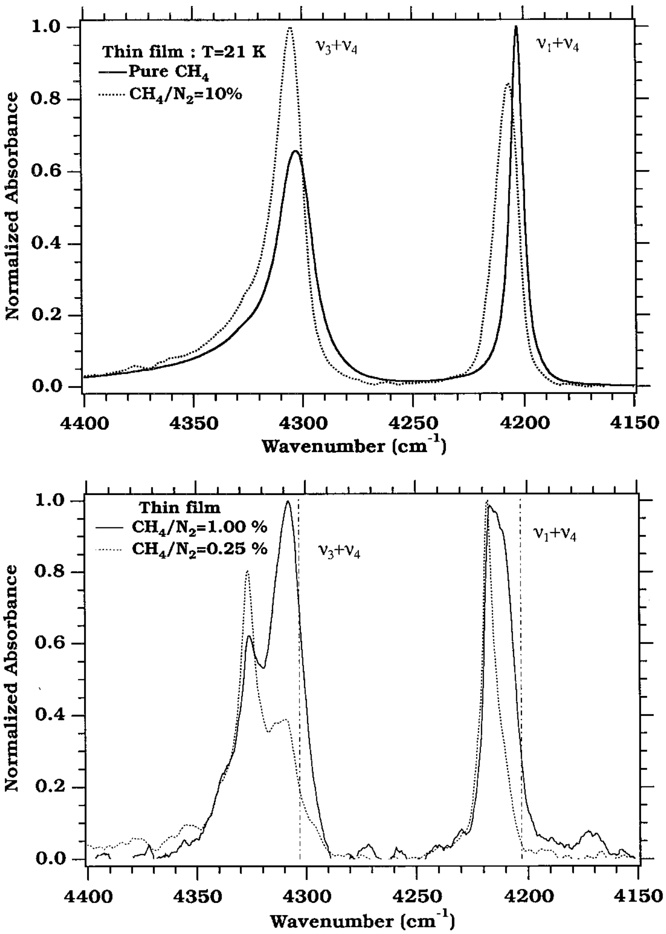

FIG. 7. Three thin-film experiments of $N_2:CH_4$ mixtures with 10, 1, and 0.25% CH_4 concentrations, exhibiting the $\nu_1 + \nu_4$ and $\nu_3 + \nu_4$ bands. For each spectrum, the peak absorbance of the strongest band has been normalized to 1.

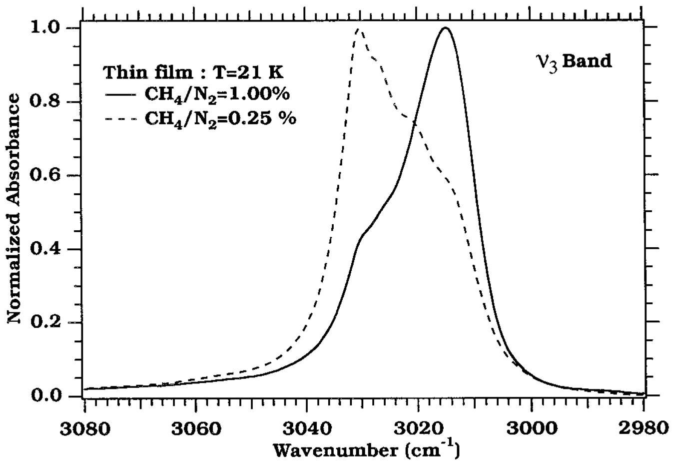

FIG. 8. ν_3 band observed for the thin-film experiments of $N_2:CH_4$ mixtures with 1 and 0.25% CH_4 concentrations. For each spectrum, the peak absorbance of the strongest band has been normalized to 1.

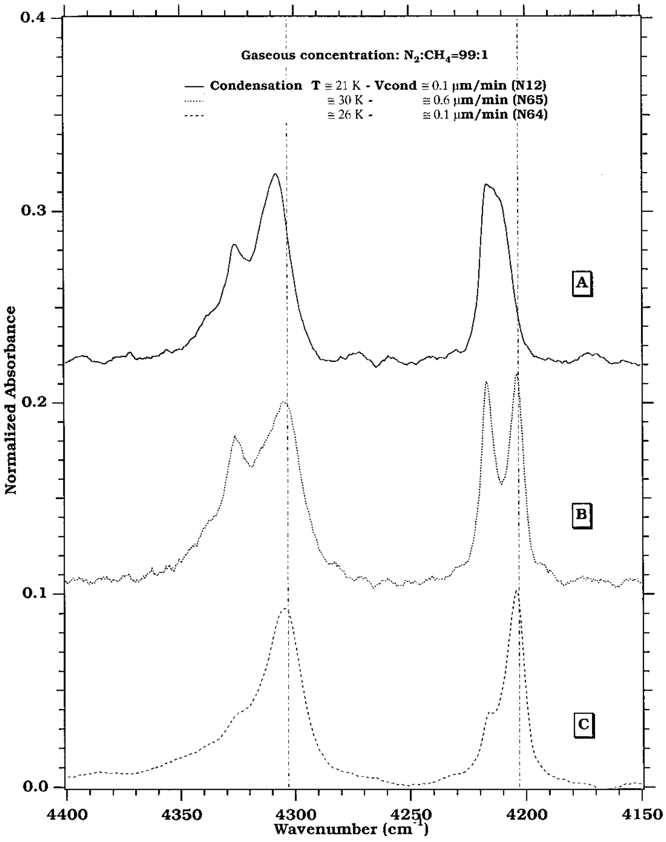

FIG. 9. Effect of experimental conditions on spectra of thin films obtained from the same gaseous mixture with 1% CH_4 concentration. The vertical dot–dash lines indicate the positions of the bands of pure CH_4 ice.

dominated by large CH_4 clusters; thus the peak positions of both bands are close to the peak positions for pure methane. The slight broadening and the different relative peak intensities could be due to contributions from smaller clusters. With the 1% CH_4 experiment, both bands show different components that could be due to the monomer and small clusters. The component at 4326 cm^{-1} of the split $\nu_3 + \nu_4$ band could be due to the monomer, and the component at 4307.8 cm^{-1} could be due to the dimer with possible contribution by other small clusters. The several components of the $\nu_1 + \nu_4$ band could also be due to the monomer and to other small clusters, which induce the shift of the band center (+9.5 cm^{-1}) and the broadening of the band. With 0.25% CH_4 in N_2, the $\nu_1 + \nu_4$ and $\nu_3 + \nu_4$ bands further changed, consistent with the previous interpretation. With decreasing concentrations, the size of the CH_4 clusters decreases and the monomer should become dominant. The component at 4326 cm^{-1} of the $\nu_3 + \nu_4$ band, assigned to the monomer, does indeed become dominant, and the $\nu_1 + \nu_4$ band is reduced to one narrow component, which should be the monomer band. Finally, comparing the ν_3 fundamental in some of our spectra with Nelander (1985), we find that the relative peak intensities of the ν_3 band in the 0.25% experiment are in agreement with a dominant monomer population.

In addition to these qualitative explanations, one can use the statistical calculations of Behringer (1958), which allow derivation of the respective numbers of different clusters in the case of a statistical mixture. Applying these calculations to the 0.25% experiment, we found that the sample should contain 98% monomers; however, this amount is not in agreement with the true cluster size distribution in the sample, which can be roughly estimated to be 80% monomers from the relative intensities of the two components of the $\nu_3 + \nu_4$ band. As a consequence, we suggest that our thin films are not exact statistical mixtures, but are in fact partly reorganized (Jödl 1989). Different chemicophysical processes probably occur during deposition (molecular diffusion, heating, etc.).

Let us now consider the question of the sensitivity of the spectra to experimental conditions (Fig. 9). Considering the $N_2:CH_4$ phase diagram (Prokhvatilov and Yantsevich, 1983), it appears that for a CH_4 concentration greater than the solubility limit (~1–2% for α-N_2 at 21 K) the $N_2:CH_4$ mixture exists as a two-phase system, i.e., CH_4-rich grains coexisting with N_2-rich grains with dissolved CH_4. It is spectroscopically possible to distinguish between the two-phase system and the solid solution, using the $\nu_1 + \nu_4$ band (Quirico *et al.* 1996). In the B experiment (Fig. 9), the $\nu_1 + \nu_4$ band clearly exhibits two components peaking at ~4216 and ~4203 cm^{-1}, which suggests the sample is a $N_2:CH_4$ two-phase system (it contains both nearly pure CH_4 and dissolved CH_4 in N_2). The same interpretation applies to the C experiment, but in this case the amount of dissolved CH_4 in N_2 with respect to nearly pure CH_4 is lower than for the B experiment. At last, experiment A seems to be a solid solution but, as previously observed, the sample contains a significant number of dimers and/or larger clusters. There are three intriguing points:

- Using different experimental conditions, one can obtain a solid solution or a two-phase system from gaseous mixtures having the same concentration (1% CH_4).
- A two-phase system can be observed for a CH_4 concentration lower than or equal to the solubility limit (1% vs 1–2%), and furthermore, the respective amount of nearly pure CH_4 with respect to dissolved CH_4 in N_2 depends on the experimental conditions.
- The solid solution contains a large amount of clusters

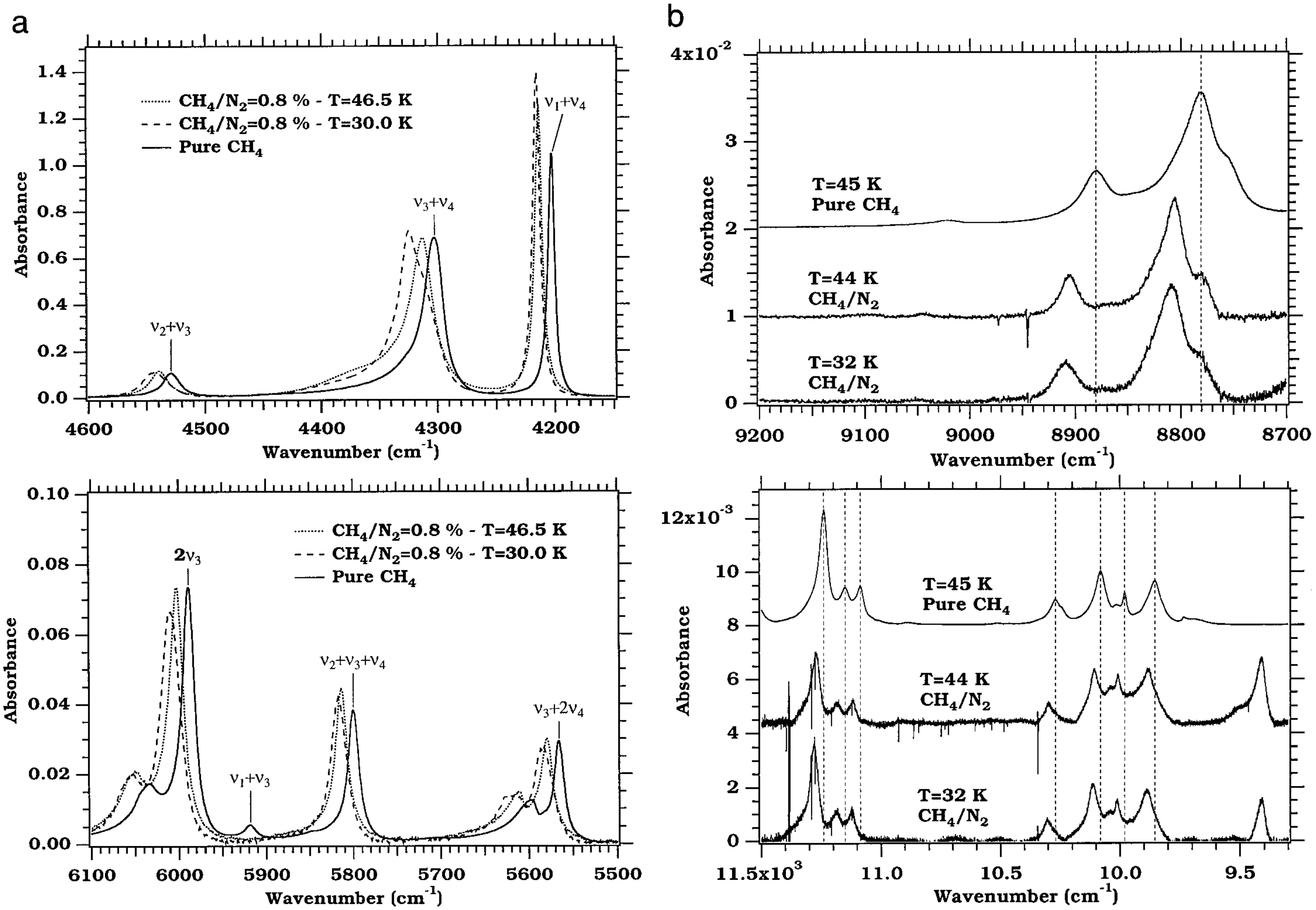

FIG. 10. (a) Dilution effect on shape, position, and intensity of vibrational bands of the CH$_4$ molecule isolated in a N$_2$ matrix, compared with pure solid CH$_4$ at 21 K (thin film). Spectra of methane diluted in N$_2$ were obtained with a 1-cm-thick crystal grown in a closed cell. (b) Same as (a), but with a pure CH$_4$ spectrum at ~45 K obtained from a sample grown in a closed cell (Grundy *et al.,* in preparation). The band at ~9410 cm^{-1} is supposed to be some impurity condensed on the exterior of the cell windows.

other than the monomer; i.e., it is inhomogeneous in terms of concentration and dilution state.

Two main explanations can be proposed. First, thin films are not formed under thermodynamical equilibrium and are, in fact, more or less reorganized statistical mixtures. The composition of a poorly reorganized sample is not consistent with the phase diagram and its spectral properties could differ considerably from those of a sample formed at thermodynamical equilibrium. This is the case in experiment A (see also Sections 4.2 and 4.3). On the other hand, more highly reorganized samples have properties much closer to those indicated by the phase diagram, which is the case in experiments B and C; however, we have yet to explain the discrepancies in the amount of nearly pure CH$_4$ with respect to dissolved CH$_4$ in N$_2$ in experiments B and C, as well as the appearance of the two-phase system at a CH$_4$ concentration lower than the solubility limit. A second process is implicated, in which molecular differentiation occurs during the deposition of the thin film. In fact, the N$_2$ and CH$_4$ molecules could have different sticking coefficients (the probability that a molecule stays stuck on the sample surface). These coefficients could depend on experimental conditions as well.

To conclude this discussion, it is necessary to compare thin-film measurements with results obtained from samples formed under conditions of thermodynamical equilibrium in a closed cell. This comparison is done in Section 4.3.

4.2. *Closed Cell Experiments*

We performed four experiments on samples grown in closed cells, at CH$_4$ concentrations of 0.1, 0.25, 0.8, and

TABLE XII
Positions of the CH_4 Bands of the Isolated CH_4 Molecule in Solid N_2, Compared with Those of Pure CH_4 Ice

Vibration mode	Pure CH_4 at 43.5 K (cm^{-1})	Diluted CH_4 in N_2 ice at 44 K (cm^{-1})	Δ (diluted-pure) (cm^{-1})
$3\nu_4$	3845.6	3856.2	+ 10.6
$\nu_2+2\nu_4$	4115.5	4126.3	+ 10.8
$\nu_1+\nu_4$	4203.2	4214.3	+ 11.1
$\nu_3+\nu_4$	4303.6	4313.4	+ 9.8
$\nu_2+\nu_3$	4528.8	4540.4	+ 11.6
$\nu_3+2\nu_4$	5565.6	5580.1	+ 14.5
$\nu_2+\nu_3+\nu_4$	5798.7	5814.7	+ 16.0
$\nu_1+\nu_3$	5919.2	------	-----
$2\nu_3$	5989.4	6003.5	+ 14.1
$\nu_2+2\nu_3$	7487.6	7506.4	+ 18.8
$2\nu_3+2\nu_4$	8587.4	8610.7	+ 23.3
$\nu_2+2\nu_3+\nu_4$	8780.75	8804.15	+ 23.4
$\nu_1+2\nu_3$	8880.2	8904.1	+ 23.9
H_2O ice (presumed)	------	9409.9	-----
$2\nu_3+3\nu_4$	9853.9	9882.2	+ 28.3
$2\nu_3+3\nu_4$	9980.0	10008.5	+ 28.5
$\nu_1+2\nu_3+\nu_4$	10080.7	10108.1	+ 27.4
$3\nu_3+\nu_4$	10269.4	10297.7	+ 28.3
$2\nu_3+4\nu_4$	11087.1	11118.3	+ 31.2
$3\nu_1+2\nu_4$	11151.1	11183.9	+ 32.8
$\nu_1+2\nu_3+2\nu_4$	11240.1	11273.5	+ 33.4

Note. Results were obtained from closed cell samples.

2% (nominal gaseous concentrations). The last experiment, at 2% CH_4, was performed using the brass cell, whereas the others were done in the first stainless-steel cell.

In the case of 0.1% CH_4, a monocrystal formed under a thermal gradient of 3 K/cm and with a cooling rate (slope of the ramp programmed in the PID controller) of 0.4 K/hr; however, this monocrystal quickly became a polycrystal on cooling. In the 0.25 and 0.8% experiments, we used large thermal gradients (12 and 24 K cm^{-1}, respectively) and a poorly controlled cooling rate and obtained polycrystals.

On cooling, we operated differently from one experiment to another, and also differently than described in Section 2. The spectra of the 0.1% CH_4 experiment were recorded while decreasing temperature for both the α and β phases. Both heaters (6) and (7) (Fig. 1) were used to limit the thermal gradient to 1 K/cm, as the large thermal inertia of the cell prevented us from controlling the temperature of the cell with only heater (7). The spectra of the 0.8% CH_4 experiment were recorded with decreasing temperature for the β phase and with increasing temperature for the α phase. On increasing the temperature, we used only the cryostat heater (when the minimum temperature was reached, we connected the PID controller to this heater). Below 30 K, we observed a thermal gradient (3 K/cm at 16.5 K) due to heat conducted into the cell along the gas inlet. The 0.25% CH_4 experiment was performed using only heater (6) (Fig. 1) and, consequently, with a large thermal gradient within the cell (24 K/cm at 60 K to about 4 K/cm at 20 K). Finally, the 2% CH_4 experiment was performed in the brass cell according to the general procedure described in Section 2.

The temperature of the sample was indirectly measured via a diode thermometer placed on the exterior of the cell. Generally, we used crystal-phase transitions (e.g., the α–β phase transition of solid N_2 at 35.6 K) to calibrate the temperature reading. If a vertical thermal gradient is present inside the cell, one has to take its presence into account as well. Because of the finite diameter of the infrared beam of the spectrometer ($\phi \sim$ 2–3 mm), the recorded spectrum will be the sum of spectra at different temperatures. For this reason, we did not keep spectra obtained with a large thermal gradient in the cell. Finally, we estimate that the temperature measurement accuracy is ±1 K for the experiment performed with the brass closed cell and ±2 K for those performed with the stainless-steel cell. For the latter cell, the greater temperature uncertainty results from the greater thermal inertia.

Finally, it must be emphasized that the absolute concentration in the sample cannot be precisely measured. A vertical concentration gradient is generally observed, and so the concentration inside the sample is inhomogeneous. We can only roughly estimate the value with respect to the concentration of the nominal gaseous mixture. In addition, during an experiment it may be necessary to move the spot of the infrared spectrometer beam, especially when the studied region becames damaged by contraction of the sample on cooling, and it is possible to choose another region that is much more transparent. In such a case, it must be pointed out that the different spectra recorded during the experiment sample regions of different concentrations.

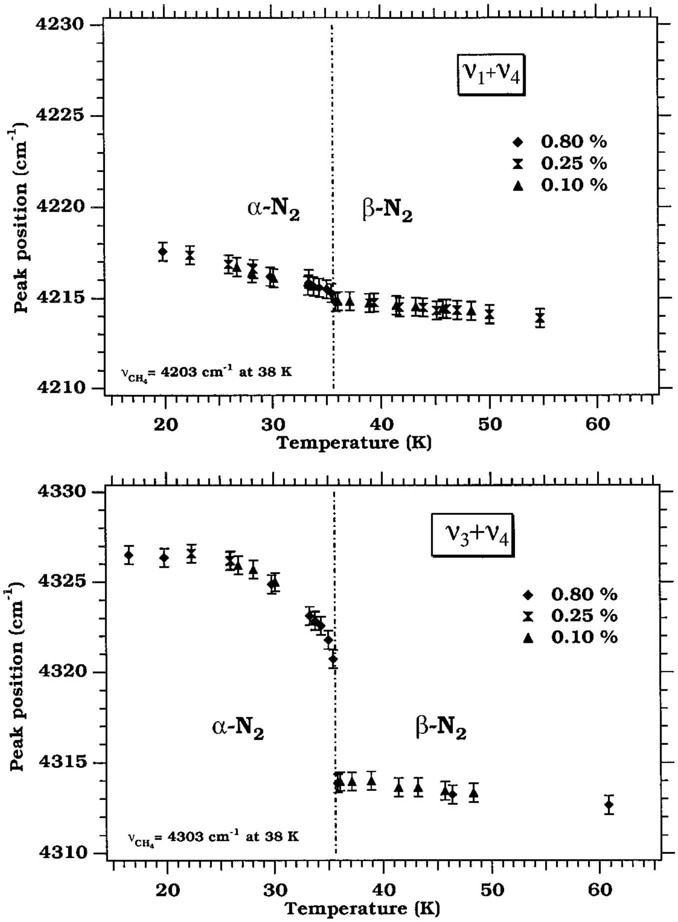

FIG. 11. Peak position of the $\nu_1 + \nu_4$ and $\nu_3 + \nu_4$ bands of the CH_4 isolated molecule in solid N_2 plotted as a function of temperature. Measurements have been performed on samples formed in the stainless-steel closed cell for 0.1, 0.25, and 0.8% CH_4 concentrations.

Experimental results. The first important result is that for four different concentrations of methane at a given temperature, the positions, contours, and relative intensities of the bands remained unchanged, and only the absolute intensity of the whole spectrum depended on concentration. This means that the concentration of CH_4 has no spectral effect within the investigated range of concentration. Moreover, it means that measurements are perfectly reproducible.

We concentrated our study on the strongest bands between 3800 and 11,500 cm^{-1} and on the weak and peculiar $\nu_1 + \nu_3$ band at 5919 cm^{-1}. Our measurements show that on dilution of N_2 ice all these bands (except $\nu_1 + \nu_3$) shift to higher frequency compared with pure methane, and the $\nu_1 + \nu_3$ band disappears (Fig. 10; Table XII). Comparing spectra of pure and diluted methane near the melting point (63.15 K), we found that the minimum value of these shifts is about 10 cm^{-1}. On cooling the shifts slowly increase, and a discontinuity (in frequency) is observed at the β–α phase transition of solid nitrogen at 35.6 K. These phase and temperature effects also operate on the shape of the bands, and their magnitude can be different from one vibration mode of the CH_4 molecule to another. Figures 11 and 12 show the temperature dependence of the band positions. In addition, no effects of diluted CH_4 were observed on the nitrogen matrix.

Another important result is that the vibron–phonon coupling band of N_2 in the fundamental region, as well as the band at 4656 cm^{-1} in the overtone region, are identical for $N_2:CH_4$ mixtures and pure N_2.

We now look in detail at the $\nu_1 + \nu_4$ and $\nu_3 + \nu_4$ bands, because they were both observed with thin-film experiments, and also they are particularly interesting from a planetological point of view (they are very well observed in Triton and Pluto spectra). The $\nu_1 + \nu_4$ band is narrow and its profile (Fig. 13) and peak frequency (Fig. 11) are poorly temperature and phase dependent ($d\nu/dT = 0.05$ cm^{-1} K^{-1} in the β phase and 0.15 cm^{-1} K^{-1} in the α phase with a frequency shift of 0.5 cm^{-1} at the phase transition). It is thus not a good temperature indicator, but provides a means of distinguishing between a solid solution and a two-phase system for the $N_2:CH_4$ mixture (Quirico *et al.* 1996). The $\nu_3 + \nu_4$ band is much stronger (Fig. 13) and its profile is significantly temperature and phase dependent (Fig. 11). Below 20 K, the $\nu_3 + \nu_4$ band presents one strong component at 4326.6 cm^{-1} and three smaller bands at 4308.8, 4315.5, and 4338.5 cm^{-1}. Above 20 K, this structure disappears and the band is asymmetric up to the phase transition of solid nitrogen at 35.6 K (Fig. 13). The peak frequency of this band is strongly temperature and phase dependent: it is almost constant up to 25 K, but decreases nonlinearly from about 4326 to 4321 cm^{-1} between 25 and 35.6 K (Fig. 11). At the phase transition, it suddenly shifts (frequency jump of about 7 cm^{-1}), and in the β phase, from 35.6 to 63.15 K, the peak frequency is not very sensitive to temperature ($d\nu/dT \sim 0.045$ cm^{-1} K^{-1}). As a consequence, the $\nu_3 + \nu_4$ band is a good temperature and phase indicator.

Discussion. By comparing the integrated intensity of several bands for the four experiments, we calculated that the concentration ratio between the 2 and 0.1% experiments was about 18 at the point selected for measurement. The concentration in the sample is different from that of the gaseous mixture due to the differentiation that occurs during crystal growth (see Section 2.2). As no spectral change was observed on increasing the concentration by a factor of 18, we conclude that in these experiments the CH_4 molecules all exist as monomers in the nitrogen matrix.

The N_2–CH_4 phase diagram (Prokhvatilov and Yantsevich 1983) shows that for low concentrations of CH_4 (less than 1–2% for the α phase and less than 3–5% below 40 K for the β phase) the N_2–CH_4 crystal is a simple solid solution. In a closed cell, a sample is formed in thermodynamical equilibrium with the liquid phase. In other words, the microscopic aspect of the crystal (solid solution vs two-phase system) should be predicted by the phase diagram. The solid solutions we observed in our cells are consistent with the phase diagram, since the CH_4 concentrations were lower than the CH_4 solubility in N_2. It is now possible to understand the perfect reproducibility of our closed cell measurements. Since all samples formed under conditions of thermodynamical equilibrium, the distribution of CH_4 in the N_2 was the same for all experiments; i.e., all CH_4 molecules exist as monomer in solid N_2. Under such conditions, the molecules in a crystal can reorganize during the crystal's growth to minimize energy, i.e., to have CH_4 molecules as widely separated as possible.

Consistent with this picture, the effects of the crystalline phase of N_2 and of temperature can be interpreted as environmental changes that perturb the motion and internal vibrational energy levels of the isolated CH_4 molecules. The phase effect could be due to the different structures of the two crystalline phases of solid nitrogen, i.e., different potential cages containing the CH_4 molecules and different dynamical interactions with the neighboring matrix molecules. Finally, the temperature effect occurs on both the position and the profile of the bands and has two main origins: (1) dependence of the volume of the unit cell of the matrix, i.e., the potential cage becoming larger or smaller, and (2) the phonon–phonon interaction (thermal agitation) (Jödl 1989). These, however, are very general explanations. More knowledge of the interactions of CH_4 with the nitrogen matrix is needed before these effects will be understood. For the moment, for planetological studies, we can fruitfully apply what we have already learned.

4.3. *Comparison between Thin Films and Closed Cell Experiments*

We now consider the intriguing discrepancies between results obtained with thin films and closed cells. Two discrepancies are particularly striking:

1. Experiments are perfectly reproducible in a closed cell and not reproducible at all with thin films.
2. Spectra are independent of CH_4 concentration with a closed cell and are dependent with thin films.

Let us consider the spectral profiles of the $\nu_1 + \nu_4$ and $\nu_3 + \nu_4$ bands, comparing the thin-film experiments at 0.25% CH_4 in N_2 with the closed cell experiment at the same temperature (Fig. 14). The slight differences (a slight shoulder on the low-frequency wing for $\nu_1 + \nu_4$, a component near 4308 cm^{-1} for $\nu_3 + \nu_4$) can be explained by the presence of clusters in the thin films, whereas inside the sample grown in a closed cell all CH_4 molecules are perfectly isolated. We note here that the thin film with 0.25% concentration is dominated by the monomer but contains small clusters, which was previously suggested by the statistical calculations of Behringer (1958). This comparison gives us a third discrepancy:

3. Perfect isolation of CH_4 is obtained in the closed cell for high concentrations (up to ~2%), whereas isolation is

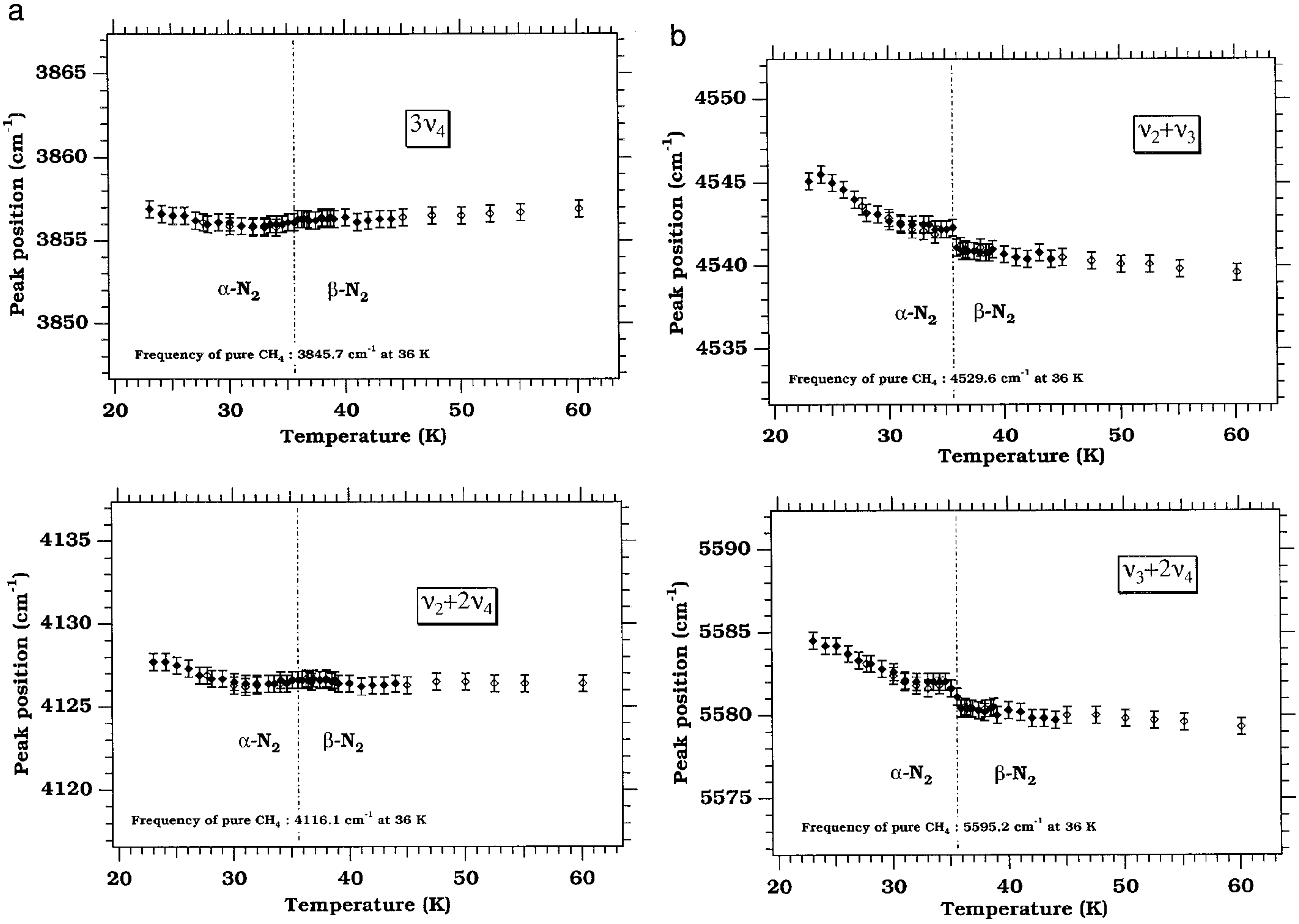

FIG. 12. Peak position of eight bands of the CH_4 molecule isolated in solid N_2 plotted as a function of temperature. Measurements have been performed on samples formed in the brass closed cell.

only partial for thin films with much lower CH_4 concentrations.

It is now possible to clarify these discrepancies in the light of the previous discussions in Sections 4.1 and 4.2. The fact that closed cell samples are formed at thermodynamical equilibrium explains both the reproducibility of the spectra and the lack of dependence on CH_4 concentration. On the other hand, the strong sensitivity of thin-film spectra to experimental conditions is due to the fact that they are partially reorganized statistical mixtures (reorganization processes directly depend on the experimental conditions) and also to differentiation occurring during the growth of the film. This differentiation effect also explains the third discrepancy. To explain the partial isolation of CH_4, it is necessary to consider that thin films are more CH_4 rich than the gaseous mixture. This enrichment can be explained by the differentiation process; i.e., CH_4 molecules stick much more efficiently than N_2 molecules. In other words, the sticking coefficient of CH_4 at 20 K would be greater than that of N_2.

5. IMPLICATIONS FOR TRITON AND PLUTO

The experimental data previously described can be used to analyze the spectra of the icy surfaces of Triton and Pluto. In particular, the systematic studies on CH_4 diluted in solid N_2 could give interesting information on the dilution state and the temperature of the surface ices of these bodies.

The first important point to discuss deals with the choice of the experimental data: thin-film vs closed cell experiments. The surfaces of Triton and Pluto are presumably

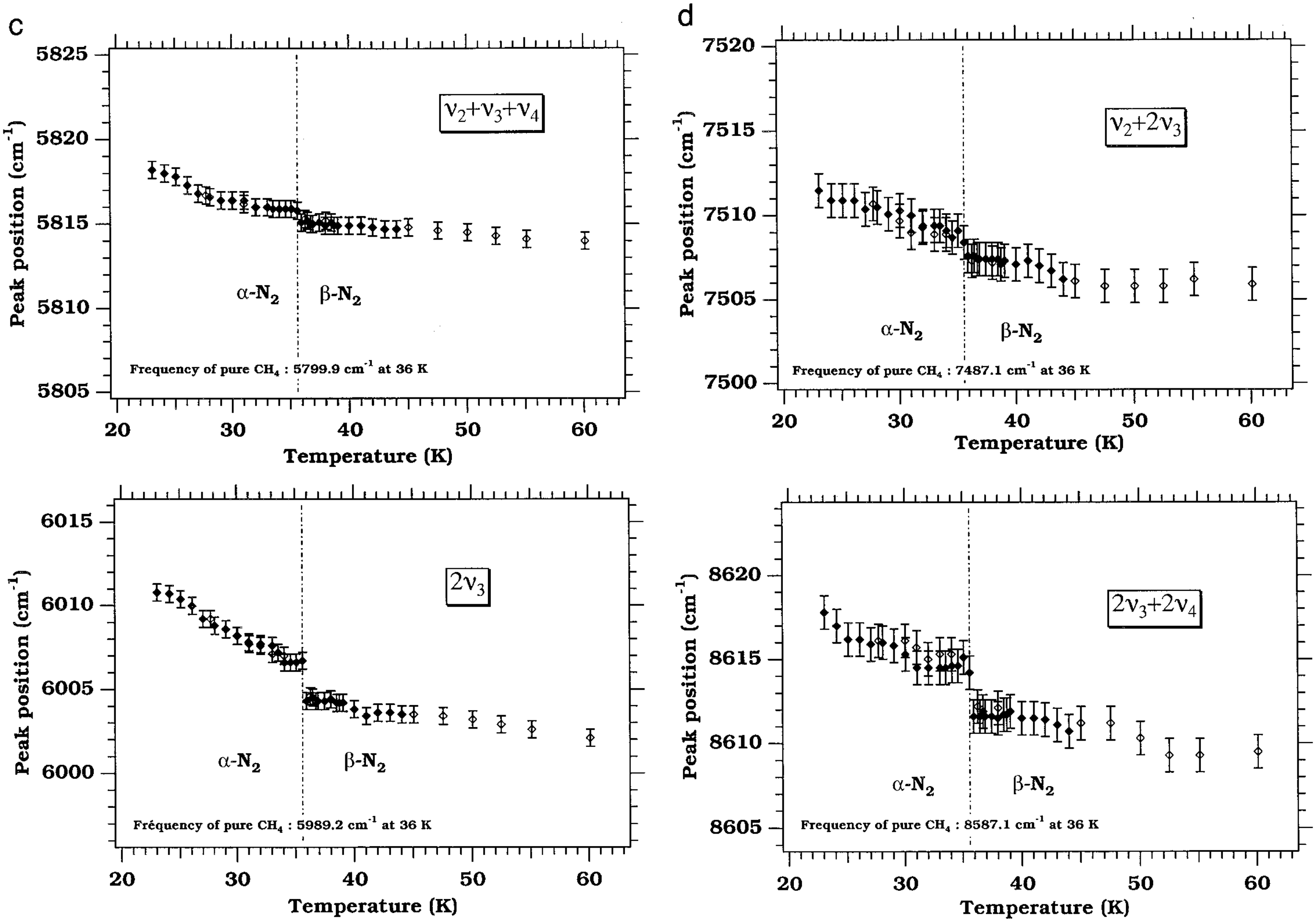

FIG. 12—*Continued*

in thermodynamical equilibrium with their atmospheres (Conrath *et al.* 1989, Broadfoot *et al.* 1989). In other words, the ices are formed by condensation of the gas under conditions of thermodynamical equilibrium. From this point of view, the closed cell experiments appear to be the preferential laboratory data to use, despite the fact that the samples are crystallized from the liquid phase. Thus, the analyses of Cruikshank *et al.* (1993) and Owen *et al.* (1993), on the basis of thin-film experiments, should be seen as a preliminary step. Further analyses should use the new laboratory data presented in this paper.

Using our data, one could expect to extract the dilution state of CH_4 and the temperature of the solid solution from telescopic data. The laboratory data clearly show that the absorption bands of CH_4 isolated in solid N_2 are shifted to higher frequencies relative to those of pure CH_4 ice. The frequency of CH_4 bands is thus a good dilution state indicator. We have also shown that the absorption bands of the isolated CH_4 molecule are temperature dependent. Thus, the peak frequency-versus-temperature curves (Figs. 11 and 12) could be used as a spectral thermometer. We also point out that the data concerning C_2H_4, C_2H_6, CO, and CO_2 molecules diluted in N_2 presented here should be used with caution because they were obtained from thin-film experiments. They can only give a rough evaluation, and new laboratory studies performed in a closed cell are necessary.

In closing, we point out that the analysis of Triton and Pluto spectra still calls for additional laboratory data. In particular, a systematic study of $N_2:CH_4$ mixtures for high CH_4 concentration is very important for Pluto and is in progress. We performed several experiments that allowed us to investigate the $N_2:CH_4$ phase diagram. These results have been very briefly presented in Quirico *et al.* (1996), and will be more completely presented in another paper. Another paper that should be published in the near future contains a systematic study of CO isolated in solid N_2. Finally, additional experimental studies will be prompted by future results obtained from ongoing observations of Triton and Pluto as well as more advanced spectral analyses.

ACKNOWLEDGMENTS

We thank Olivier Brissaud for having designed and built the cyogenic cells, and Roberto Bini for his help from both experimental and theoretical points of view. We are grateful to Alessandro Nucara and Paolo Calvani for stimulating discussions on solid methane spectroscopy, and also Jean-Pierre Hilico for communicating results from his theoretical calculations on the isolated CH_4 molecule. We particularly thank Dale Cruikshank, Tobias Owen, and Catherine de Bergh for their encouragements to pursue this work, and their patience in reading it as a published paper! We are also very grateful to Will Grundy who checked the English language of the text. Finally, we particularly thank two anonymous reviewers for fructuous comments and suggestions which increase the quality of the paper. This research was supported by the Programme National de Planétologie from the French Institut National des Sciences de l'Univers. Eric Quirico acknowledges a grant from the French Ministère de la Recherche et de l'Enseignement Supérieur.

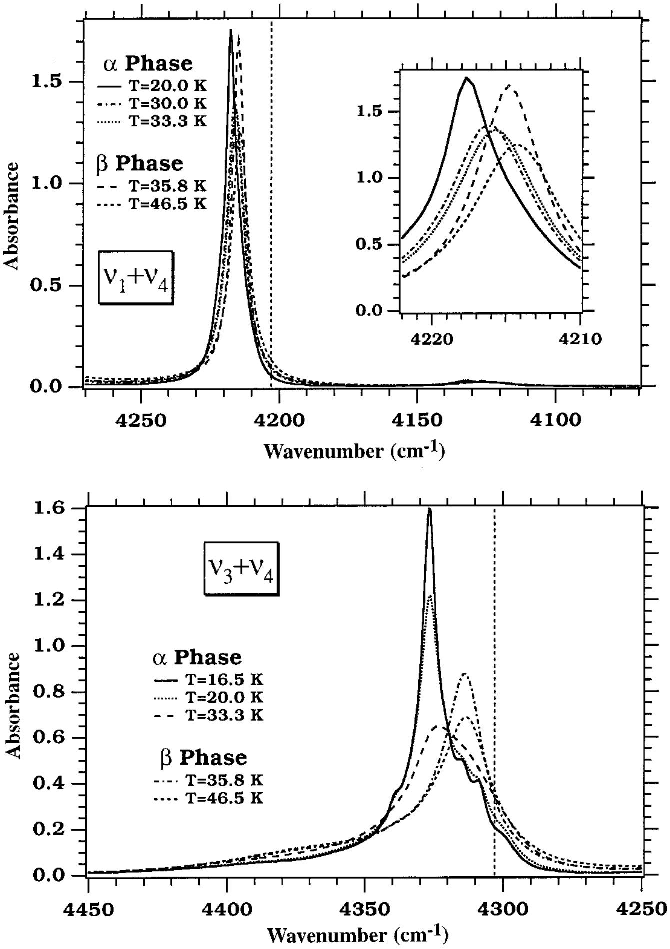

FIG. 13. Temperature and phase effect on the spectral profile of the $\nu_1 + \nu_4$ and $\nu_3 + \nu_4$ bands of the CH_4 isolated molecule in solid N_2. Measurements have been performed on samples formed in the stainless-steel closed cell, for a given concentration of the sample. The absorbance has not been renormalized.

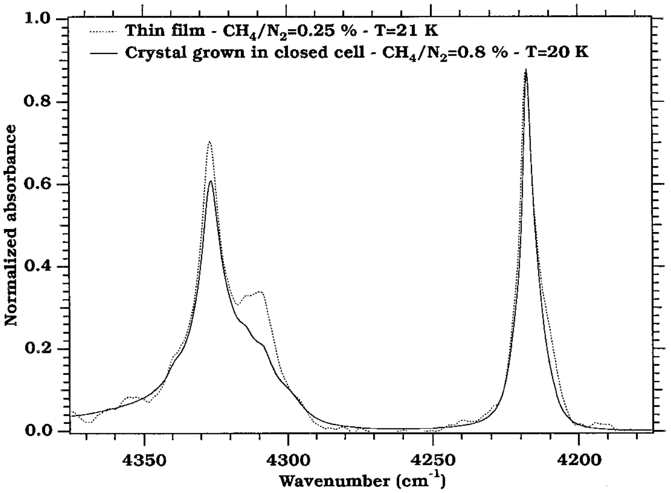

FIG. 14. Effect of formation process: Comparison of spectra obtained respectively in a closed cell and with thin-film technique. For both spectra, the absorbance of the strongest $\nu_1 + \nu_4$ band has been artificially normalized to 1.

REFERENCES

Baciocco, G., P. Calvani, and S. Cunsolo 1987. Weak infrared bands in solid CH_4-II. *J. Chem. Phys.* **87,** 1913–1916.

Baran, B. W., and F. D. Medina 1986. Far-infrared spectrum of solid methane. Phase II. *Chem. Phys. Lett.* **129,** 125–129.

Behringer, R. E. 1958. Number of single, double, and triple clusters in a system containing two types of atoms. *J. Chem. Phys.* **29,** 537–539.

Bini, R., H. J. Jödl, and S. Califano 1992. Relaxation processes of the infrared-active lattice phonons of crystalline CO_2. *Phys. Rev. B* **45,** 5244–5250.

Bini, R., P. R. Salvi, V. Schettino, and H. J. Jödl 1993. The spectroscopy and relaxation dynamics of three-phonon bound states in crystal CO_2. *J. Chem. Phys.* **98,** 164–177.

Brecher, C., and R. S. Haldford 1961. Motions of molecules in condensed systems. XI. Spectrum and structure of a single crystal of ethylene. *J. Chem. Phys.* **35,** 1109–1117.

Brith, M., and A. Ron 1969. Far-infrared spectra of crystalline C_2H_4 and C_2D_4. *J. Chem. Phys.* **50,** 3053–3056.

Broadfoot, A. L., S. K. Atreya, J. L. Bertaux, J. E. Blamont, A. J. Dessler, T. M. Donahue, W. T. Forrester, D. T. Hall, F. Herbert, J. B. Holberg, D. M. Hunten, V. A. Krasnopolsky, S. Linick, J. I. Lunine, J. C. McConnell, H. W. Moos, B. R. Sandel, N. M. Schneider, D. E. Shemansky, G. R. Smith, D. F. Strobel, and R. V. Yelle 1989. Ultraviolet spectrometer observations of Neptune and Triton. *Science* **246,** 1459–1466.

Cabana, A., G. B. Savitsky, and D. F. Hornig 1963. Vibration–rotation spectra of CH_4 and CD_4 impurities in xenon, krypton and argon crystals. *J. Chem. Phys.* **39,** 2942–2950.

Calvani, P., S. Cunsolo, S. Lupi, and A. Nucara 1992. The near-infrared spectrum of solid CH_4. *J. Chem. Phys.* **96,** 7372–7379.

Cardini, G., R. Righini, H. W. Löwen, and H.-J. Jödl 1992. Sideband modeling in molecular crystals N_2 and CO_2. *J. Chem. Phys.* **96,** 5703–5711.

Carr, B. R., B. M. Chadwick, C. S. Edwards, D. A. Long, and F. C. Wharton 1980. The infrared activation of the N–N stretching vibration in nitrogen matrices. *J. Mol. Struct.* **62,** 291–295.

Chamberland, A., R. Belzile, and A. Cabana 1970. Infrared spectra and structure of methane–noble gas mixed crystals: The influence of temperature and methane concentration on the ν_3 vibration band of methane. *Can. J. Chem.* **48,** 1129–1139.

Chapados, C., and A. Cabana 1972. Infrared spectra and structures of solid CH_4 and CD_4 in phases I and II. *Can. J. Chem.* **50,** 3521–3533.

Collins, S. T., P. A. Casey, and G. C. Pimentel 1988. The IR spectrum of ethylene in solid xenon: Host–guest mode coupling. *J. Chem. Phys.* **88,** 7307–7311.

Conrath, B., F. M. Flasar, R. Hanel, V. Kunde, W. Maguire, J. Pearl, J. Pirraglia, R. Samuelson, P. Gierasch, A. Weir, B. Bézard, D. Gautier, D. Cruikshank, L. Horn, R. Springer, and W. Schaffer 1989. Infrared observations of the Neptune system. *Science* **246,** 1454–1459.

Cruikshank, D. P., T. L. Roush, T. C. Owen, T. R. Geballe, C. de Bergh, B. Schmitt, R. H. Brown, and M. J. Bartholomew 1993. Ices on the surface of Triton. *Science* **261,** 742–745.

Di Lella, D. P., and D. E. Tevault 1986. Infrared absorption of solid nitrogen activated by CO_2, H_2O and C_2N_2. *Chem. Phys. Lett.* **126,** 38–42.

Dows, A. D. 1962. Infrared spectra of crystalline C_2H_4 and C_2D_4. *J. Chem. Phys.* **36,** 2833–2835.

Dubost, H. 1976. Infrared absorption spectra of carbon monoxide in rare gas matrices. *Chem. Phys.* **12,** 139–151.

Dubost, H., and L. Abouaf-Marguin 1972. Infrared spectra of carbon monoxide trapped in solid argon. Double-doping experiments with H_2O, NH_3 and N_2. *Chem. Phys. Lett.* **17,** 269–273.

Dubost, H., R. Charneau, and M. Harig 1982. High-resolution diode laser spectroscopy of CO in solid N_2: Effect of dipolar broadening on vibrational transitions. *Chem Phys.* **69,** 389–405.

Ewing, G. E. 1962. Infrared spectra of liquid and solid carbon monoxide. *J. Chem. Phys.* **37,** 2250–2256.

Ewing, G. E. 1964. Infrared absorption of the ν_3 fundamental of liquid and solid CH_4 and CD_4. *J. Chem. Phys.* **40,** 179–183.

Ewing, G. E., and G. C. Pimentel 1961. Infrared spectrum of solid carbon monoxide. *J. Chem. Phys.* **35,** 925–930.

Falk, M. 1987. Amorphous solid carbon dioxide. *J. Chem. Phys.* **86,** 560–564.

Fink, U., and G. T. Sill 1982. The infrared spectral properties of frozen volatiles. In *Comets* (L. L. Wilkening, Ed.), pp. 164–202. University of Arizona Press, Tucson.

Foggi, P., and V. Schettino 1992. Phonon relaxation in molecular crystals: Theory and experiments. *Riv. Nuov. Cim. Soc. Fis.* **7**.

Fredin, L., B. Nelander, and G. J. Ribbegard 1974. On the dimerization of carbon monoxide in nitrogen and argon matrices. *J. Mol. Spectrosc.* **53,** 410.

Green, J. R., R. H. Brown, D. P. Cruikshank, and V. Anicich 1991. The absorption coefficient of nitrogen with application to Triton. *Bull. Am. Astron. Soc.* **23,** 1208 (abstract).

Grundy, W. M., B. Schmitt, and E. Quirico 1993. The temperature dependent spectra of α and β nitrogen ice with application to Triton. *Icarus* **105,** 254–258.

Hansen, G. B. 1992. The spectral absorption of CO_2 ice from 0.18 to 4.8 μm. *Bull. Am. Astron. Soc.* **24,** 978 (abstract).

Herzberg, G. 1948. *Infrared and Raman Spectra of Polyatomics Molecules.* Van Nostrand, New York.

Hilico, J.-C., J.-P. Champion, S. Tonmi, V. G. Tynterev, and S. A. Tashkun 1994. New analysis of the pentad system of methane and prediction of the spectrum. *J. Mol. Spectrosc.* **168,** 455–476.

Hilico, J.-C., S. Tonmi, and L. R. Brown 1995. The octad of interacting vibrational states of methane. *Astron. Soc. Pac. (ASP) Conf. Ser.* **81,** 322–324.

Irvine, M. J., J. G. Mathieson, and A. D. E. Pullin 1982. The infrared matrix isolation of carbon dioxide. II. Argon matrices: The CO_2 monomer bands. *Aust. J. Chem.* **35,** 1971–1977.

Jödl, H. J. 1989. Solid-state aspects of matrices. In *Chemistry and Physics of Matrix-Isolated Species* (L. Andrews and M. Moskovits, Eds.), Chap. 12. North-Holland, Amsterdam.

Khare, B. N., W. R. Thompson, C. Sagan, E. T. Arakawa, C. Bruel, J. P. Judish, R. K. Khanna, and J. B. Pollack 1990. Optical constants of solid methane. In *First International Conference on Laboratory Research for Planetary Atmospheres* (K. Fox, J. E. Allen, L. J. Stief, and D. T. Quillen, Eds.). *NASA Conf. Publ.* **3077,** 327–339.

Legay, F., and N. Legay-Sommaire 1982. Vibrational absorption spectrum of solid CO in the first harmonic region. Two-phonon transition. *Chem. Phys.* **65,** 49–57.

Legay, F., and N. Legay-Sommaire 1996. Simultaneous vibrational excitations in solid α-nitrogen in the 4600–4700 cm^{-1} region. *Chem. Phys.,* in press.

Legay-Sommaire, N., and F. Legay 1982. Analysis of the infrared emission and absorption spectra from isotopic CO molecules in solid α-CO. *Chem. Phys.* **66,** 315–325.

Leroi, G. E., G. E. Ewing, and G. C. Pimentel 1964. Infrared spectra of carbon monoxide in an argon matrix. *J. Chem. Phys.* **40,** 2298–2303.

Llewellyn, H. J., S. A. Ekberg, and B. I. Swanson 1986. Hindered rotation and site structure of methane trapped in rare gas solids. *J. Chem. Phys.* **85,** 3203–3210.

Löwen, H. W., K. D. Bier, H. J. Jödl, A. Löwenschuss, and A. Givan 1989. The vibron–phonon sidebands in the Fourier-transform infrared spectra of the molecular crystal CO_2. *J. Chem. Phys.* **90,** 5309–5314.

Löwen, H. W., K. D. Bier, and H. J. Jödl 1990. Vibron–phonon excitations in the molecular crystals N_2, O_2 and CO by Fourier transform infrared and Raman studies. *J. Chem. Phys.* **93,** 8565–8575.

Nelander, B. 1976. On the infrared spectrum of a carbon dioxide containing nitrogen matrix. *Chem. Phys. Lett.* **42,** 187–189.

Nelander, B. 1985. An infrared spectroscopic study of the rotation of methane in solid nitrogen. *J. Chem. Phys.* **82,** 5340–5345.

Owen, T. C., T. L. Roush, D. P. Cruikshank, J. L. Elliot, L. A. Young, C. de Bergh, B. Schmitt, T. R. Geballe, R. H. Brown, and M. J. Bartholomew 1993. Surface ices and the atmospheric composition of Pluto. *Science* **261,** 745–748.

Pearl, J., M. Ngoh, M. Ospina, and R. Khanna 1991. Optical constants of solid methane and ethane from 10000 to 450 cm^{-1}. *J. Geophys. Res.* **96,** 477–482.

Prokhvatilov, A. I., and L. D. Yantsevich 1983. X-ray investigation of the equilibrium phase diagram of CH_4–N_2 solid mixtures. *Sov. J. Low Temp. Phys.* **9,** 94–98.

Quirico, E., and B. Schmitt 1997. A spectroscopic study of CO diluted in solid N_2: Implications for Triton and Pluto. *Icarus,* in press.

Quirico, E., B. Schmitt, R. Bini, and P. R. Salvi 1996. Spectroscopy of some ices of astrophysical interest: SO_2, N_2 and N_2:CH_4 mixtures. *Planet. Space Sci.* **44,** 973–986.

Roux, J. A., B. E. Wood, A. M. Smith, and R. R. Plyler 1980. *Infrared Optical Properties of Thin CO, NO, CH_4, HCl, N_2O, O_2, N_2, Ar and*

Air Cryofilms. Arnold Engineering Development Center Report AEDC-TR-79-81.

Rytter, E., and D. M. Gruen 1979. Infrared spectra of matrix isolated and solid ethylene. Formation of ethylene dimers. *Spectrochim. Acta A* **35,** 199–207.

Savoie, R., and R. P. Fournier 1970. Far-infrared spectra of condensed methane and methane-d_4. *Chem. Phys. Lett.* **7,** 1–3.

Scheidt, A. 1993. *FTIR spektroskopie in Ar : N_2 untersuchungen der hexagonalen phase und des orientierungsglases.* Diplomarbeit in Experimentalphysik, Universität Kaiserslautern.

Schmitt, B., A. Oehler, R. Calvier, P. Haschberger, and E. Lindermeier 1990. The near infrared absorption features of solid nitrogen and methane on Triton. *Bull. Am. Astron. Soc.* **22,** 1121 (abstract).

Schmitt, B., E. Quirico, and E. Lellouch 1992. Near infrared spectra of potential solids at the surface of Titan. In *Proceedings, Symposium on Titan. ESA Spec. Publ.* **SP-338,** 383–388.

Schwartz, Y. A., A. Ron, and S. Kimel 1971. Far-infrared spectra of ethane, ethylene and acethylene. *J. Chem. Phys.* **54,** 99–105.

Scott, T. A. 1976. Solid and liquid nitrogen. *Phys. Rep.* **27,** 87–157.

Tejada, S. B., and D. F. Eggers 1976. Infrared spectra of ordered crystalline ethane and ethane-d_6. *Spectrochim. Acta A* **32,** 1557–1562.

Tryka, K. A., R. H. Brown, V. Anicich, D. P. Cruikshank, and T. C. Owen 1993. Spectroscopic determination of the phase composition and temperature of nitrogen ice on Triton. *Science* **261,** 751–754.

Tryka, K. A., R. H. Brown, and V. Anicich 1995. Near-infrared coefficients of solid nitrogen as a function of temperature. *Icarus* **116,** 409–414.

Tyler, G. L., and 17 co-authors 1989. Voyager radio science observations of Neptune and Triton. *Science* **246,** 1466–1473.

Warren, S. G. 1986. Optical constants of carbon dioxide ice. *Appl. Opt.* **25,** 2650–2674.

Wisnosky, M. G., D. F. Eggers, L. R. Fredrickson, and J. C. Decius 1983a. The vibrational spectra of solid II ethane and ethane-d_6. *J. Chem. Phys.* **79,** 3505–3512.

Wisnosky, M. G., D. F. Eggers, L. R. Fredrickson, and J. C. Decius 1983b. A metastable solid phase of ethane. *J. Chem. Phys.* **79,** 3513–3516.